This is a peer-reviewed, accepted author manuscript of the following research article: Ogbeifun, A., Oterkus, S., Race, J., Naik, H., Moorthy, D., Bhowmik, S., & Ingram, J. (Accepted/In press). Simulation stage-based seabed pre-trenching technique for steel catenary riser touchdown fatigue analysis. *Ships and Offshore Structures* . https://doi.org/10.1080/17445302.2021.1999040

Simulation Stage-Based Seabed Pre-Trenching Technique for Steel Catenary Riser Touchdown Fatigue Analysis

Achoyamen Ogbeifun[a*], Selda Oterkus[a], Julia Race[a],
Harit Naik[b], Dakshina Moorthy[c], Subrata Bhowmik[b], Julie Ingram[c]

[a]*Naval Architecture, Ocean and Marine Engineering, University of Strathclyde, Glasgow, G4 0LZ, UK*
[b]*McDermott International, 40 Eastbourne Terrace, Paddington, London, W2 6LG, UK*
[c]*McDermott International, 757 N. Eldridge Parkway, Houston, TX 77079, USA*

Abstract

The development of seabed trench by the steel catenary riser (SCR) touch down zone (TDZ) in its early life can be caused by installation loads, direct hydrodynamic loads and vessel first and second-order motion imposed on the SCR during and after its installation. Several studies have been conducted to investigate the SCR TDZ fatigue response as the excited SCR TDZ progressively trench itself into the seabed, while other studies have investigated the impact of existing trench or pre-trench on the SCR fatigue response. However, most of these investigations were conducted using a series of regular wave loads through quasi-static simulations. Also, though important information on the trench effect on SCR TDZ fatigue response is known in the research domain, little has been said about how to incorporate them in the actual riser design process. This paper (part 1) presents a numerical technique by which pre-trench can be initiated for fatigue response calculations during SCR detailed design analysis. Examples are presented to demonstrate the new approach and how the SCR fatigue response can be calculated in the presence of the created pre-trench. The SCR (after the pre-trenching process) is allowed to respond to the vessel first order six degrees of freedom motions about its nominal position in the presence of the created pre-trench. As demonstrated in this paper, the pre-trenching technique makes it possible to conduct a full time-domain, irregular wave simulations of the SCR in the presence of a pre-trench created using the hysteretic non-linear pipe soil interaction model.

Keywords: Steel Catenary Risers; Touch Down Zone; Fatigue Damage Response; Pre-trench; Time History; Simulation Stage.

Introduction

Steel catenary risers (SCRs) are the most applied type of risers systems in deepwater field development for the transportation of production-related materials between the seabed and the host floating platform (Song and Stanton) (Clukey, Ghosh, et al.). The wide application of SCR is attributed to its simplicity, relatively lower procurement cost, easy installation and maintenance (Quintin et al. 2007) (Quéau et al. 2015). However, it can be challenging to implement SCR in a very harsh environment and on floating platforms characterised by high motions. This is because the resulting dynamic loads imposed on SCR cause high stresses and fatigue damage around its critical sections, which are the touchdown zone (TDZ) and hang off (HO) (Gore and Mekha 2002). The TDZ is the dynamic section of the SCR in contact with the seabed. This is the section that is actively entrenched into the seabed when the riser is excited. As observed from field data, the trench vertical inline geometries are mostly ladled in shape (Bridge and Howells 2007), with the trench deepest near the trench mount (between the catenary zone and the buried zone) shown in Figure 1. The transverse geometry (not shown here) has a bell mouth shape, which is widest near the trench mount and tappers to the riser pipe bearing width near the surface zone.

*Corresponding author. Tel.: +44 7414517860.
E-mail address: achoyamen.ogbeifun@strath.ac.uk, genmik@yahoo.com

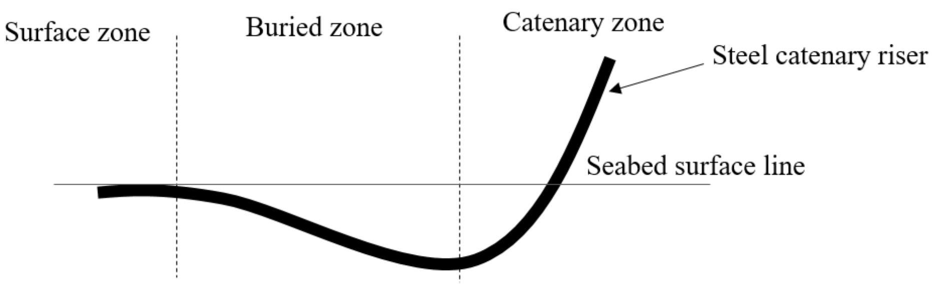

Figure 1 – Schematic of seabed trench geometry created by active SCR TDZ (along the riser plane)

The strength and fatigue responses of SCR around the TDZ is dependent on its interaction with the seabed. Realistically, the riser-seabed interaction is non-linear, with operative soil stiffness varying with the riser displacement amplitude (Mekha et al. 2013). However, it is a long design practice in the riser industry to simplify the seabed interaction model as rigid or elastic. This simplistic approach does not sufficiently provide an accurate basis for accessing the fatigue damage around SCR TDZ (Zargar et al. 2019). The wrong prediction of SCR responses can significantly impact its structural design limit, safety, and cost. It is therefore imperative to increase the understanding of the non-linear interactions of the SCR and the seabed.

SCR soil interactions assessment has been a major subject for the riser industry and research institutions (Clukey, Aubeny, et al.). Many kinds of research have been conducted to improve on the riser soil interaction models, resulting in several non-linear (NL) numerical models used to approximate the real riser seabed interactions (Aubeny and Biscontin 2009, Randolph and Quiggin 2009, Zargar, Kimiaei and Randolph 2019). These NL riser soil interaction models have helped researchers to increase understanding of the SCR TDZ fatigue behaviour. An example of these NL interaction models (used in this paper) is the model proposed by Randolph and Quiggin (RQ) for an SCR TDZ oscillating under dynamic loading conditions (Randolph and Quiggin 2009). The RQ model has been implemented in OrcaFlex, an offshore dynamic software widely used in the industry and academic domain (Orcina 2018). The RQ model penetration modes and characteristics are shown in Figure 2. The model captures the non-linear behaviour of the soil as it is deformed by the motions of the SCR TDZ travelling through it. The non-linearity captured during the SCR TDZ inversions include soil stiffness degradation under cyclic loading, soil suction resistance and the soil buoyancy force on the SCR TDZ. Details of the RQ model can be found in (Randolph and Quiggin 2009).

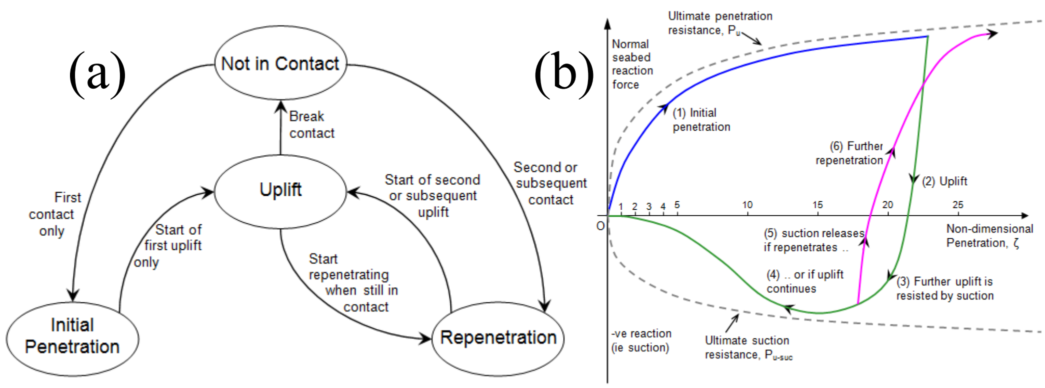

Figure 2 – Non-linear hysteretic pipe soil interaction model (Randolph and Quiggin 2009): (a) penetration modes, (b) characteristics for different modes as modified in (Orcina 2018)

The ROV survey conducted during the STRIDE JIP on three fields – Allegheny Green Canyon in the Gulf of Mexico (GoM), Marlin in GoM and P18 Marlim in Compos Basin, showed that stabilised trenches of several riser pipe diameters (OD) were created and that the SCR TDZs were entrenched in them (Bridge and Howells 2007). The period in which these trenches developed were relatively short compared to the design life cycle of the riser system. Hence, the trench can be considered as a pre-trench prior to the operational life cycle of the riser system and should be included in the SCR fatigue analysis. Therefore, there is the need to develop robust techniques to create an explicit trench for SCR fatigue analysis

A number of authors proposed the use of some mathematical functions to model initial trench (Giertsen et al. 2004, Langner 2003, Mekha, Randolph, Bhat and Jain 2013, Sharma and Aubeny 2011, Wang and Low 2016). For example, Langner (2003) investigated the pre-trench impact on the fatigue TDZ response using a circular arc to fit the riser side of the TDZ and a seventh order polynomial to set the boundary conditions for the pipeline side. It was concluded that the trench was positive to the SCR fatigue life. An investigation conducted by Sharma and Aubeny (2011) employed the cyclic riser seabed interaction model developed by Aubeny and Biscontin (2009) to incrementally create pre-trench. The final numerical trench was then modified using cubic polynomials to fit either side of the trench from the deepest point. The study concluded that the pre-trench has a positive impact on SCR fatigue life. A numerical investigation was conducted by Shiri and Randolph (2010), using the RQ model to effect incremental SCR TDZ embedment to an ultimate trench condition in which the SCR TDZ fatigue response was investigated. The results showed that the pre-trench condition increases the SCR TDZ fatigue damage.

From these investigations and many others (not mentioned here), conflicting reports exist on the impact of the pre-trench on the SCR TDZ fatigue response. For example, while some authors reported that the trench increases fatigue damage (Rezazadeh et al. 2012, Shiri 2014a, Shiri 2014b, Shiri and Randolph 2010), others have a contrary conclusion (Elliott et al. 2013, Langner 2003, Mekha, Randolph, Bhat and Jain 2013, Nakhaee and Zhang 2008, Sharma and Aubeny 2011). The major challenge with pre-trench modelling and analysis is the danger of pressure hot spots being generated along the SCR TDZ section in contact with the pre-trench wall, resulting in unrealistic fatigue prediction (Mekha, Randolph, Bhat and Jain 2013, Shoghi and Shiri 2020). This was observed by Shoghi and Shiri (2020), who reviewed some existing literature on the subject and attributed the confliction in reports to a possible abnormality in the pre-trenching process. Unrealistic fatigue damage may result from an incompatible trench and the embedded SCR TDZ natural profiles (Shoghi and Shiri 2020).

Also, many of these investigations have applied regular wave loads and significant simplifications in the analysis process. Therefore, it is essential to advance the pre-trench modelling process to create a more realistic pre-trench envelope for SCR TDZ fatigue investigation. A natural and fully developed pre-trench can be achieved by exciting the SCR TDZ through the vessel's first and second-order wave load and slow vessel drift motion during the lifetime of the SCR (Shoghi and Shiri 2020). Such a fully developed trench will have a longer span (along the riser plane) and depth to accommodate the SCR TDZ motions.

One of the advanced techniques developed to address the pressure hot spots in the pre-trench profile is the "stepped trench" technique (Mekha, Randolph, Bhat and Jain 2013). The technique is a numerical-analytic method, which starts with a base trench profile generated numerically (Shiri and Randolph 2010) (see Figure 3 (a)). The base trench is then modified analytically such that the profile is identical to the riser profile on the pipeline side (see section 1 of Figure 3 (b)). On the riser side, the trench profile is made a mirror image of the pipeline side up to the point of inflexion (see section 2 of Figure 3 (b)), and then extrapolated linearly beyond (see section 3 of Figure 3 (b)). The modifications intend to expand the trench envelope to accommodate all motions of the SCR TDZ resulting from vessel excursions. However, it is not clear if this was achieved throughout the loading cycles of the analysis. With the current capability of OrcaFlex, it may be difficult to replicate the analytically modified trench profile for time-domain fatigue analysis of the SCR.

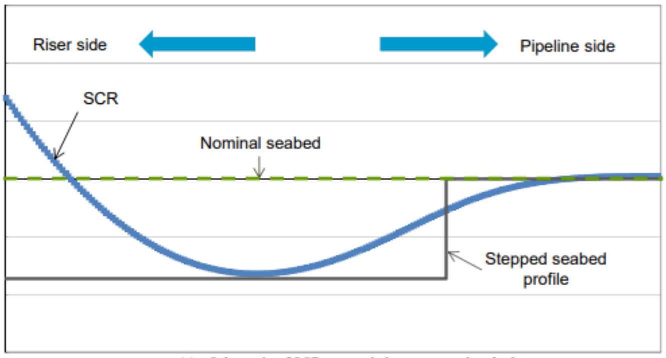

(a) Schematic of SCR suspended over stepped seabed

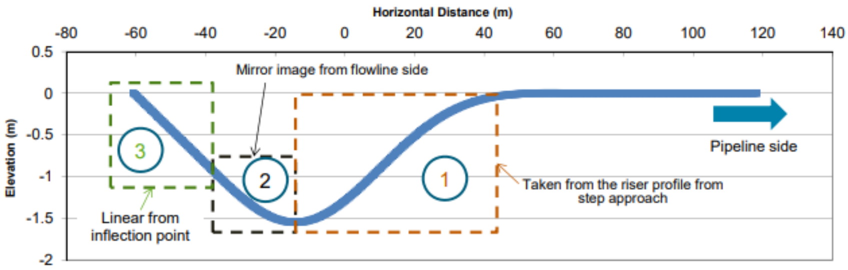

(b) Construction of trench profile

Figure 3 – Stepped trench profile development (Mekha, Randolph, Bhat and Jain 2013)

There is a need in the riser industry, during SCR design analysis, to be able to initiate a pre-trench and quantify its impact on the SCR TDZ response during the simulation of complex loading conditions in a full-time domain. A new numerical technique is presented in this paper, referred to as the simulation stage-based pre-trenching technique (SSBPT). The development of the SSBPT follows the guidelines suggested in (Shoghi and Shiri 2020) to enhance the correctness of the pre-trench analysis. These include the vessel excursion in the pre-trenching process, ensuring the created pre-trench profiles accommodate the SCR TDZ motions, and post-processing fatigue response results through the active TDZ sections rather than selected nodes. The new technique uses the incremental trench capability of the RQ pipe soil interaction model to create an explicit trench to which the riser is subjected in time domain fatigue simulation. The trenching process will include the vessel first order motions and oscillatory offsets (representing second-order vessel drift) about the vessel's nominal position.

1. Numerical Trenching Methodology

1.1. Simulations stage based pre-trenching technique

The early method of conducting fatigue analysis assumes that the SCR TDZ lie on infinite stiff soil. This means no seabed penetration during the SCR TDZ excitations, but only pipe stress generated due to the active contact between SCR TDZ and the seabed. This assumption, although conservative, is not correct, hence the development of the linear (Spring model) and subsequently the more advanced non-linear SCR-soil interaction model (e.g. the RQ model). The RQ model represents finite soil stiffnesses and models the pipe inversions in the seabed. The model is developed on the backbone curve, which provides considerable stiffness resistance to the pipe penetration at the beginning of the loading cycle. Hence, small vessel excitations (typical of fatigue loads) can only cause negligible pipe penetration. This is a limitation of the RQ model and makes it challenging to create a pre-trench explicitly. However, even within these negligible penetrations, the hysteretic pipe - soil interactions are still represented. The pipe either remains in contact with the seabed, where the hysteretic stiffness exists or breaks out from the seabed contact for large enough upward riser motions. The SSBPT provided in this paper to generate deeper trenches is built on the RQ model's capabilities. This is achieved using large regular wave loads, the first-order vessel motions and oscillatory vessel offsets (second-order drifts).

For the SSBPT, the simulation stage is decomposed into three stages, namely the trenching stage, the rest stage and the main stage, as shown in Figure 4. The load applied during the trenching stage is referred to as the trenching load, and the length of time over which the load is applied is referred to as the trenching period. Once the desired trench envelope is reached, the trenching load is discontinued, and the system is allowed to transit through a resting stage where the system achieves dynamic calmness prior to the main stage simulation. The fatigue load is then imposed during the main stage simulation. In each of the stages, the vessel motion responses are expressed as time histories. The time histories of the three stages are then composed as single time history and imposed on the vessel in a single simulation run.

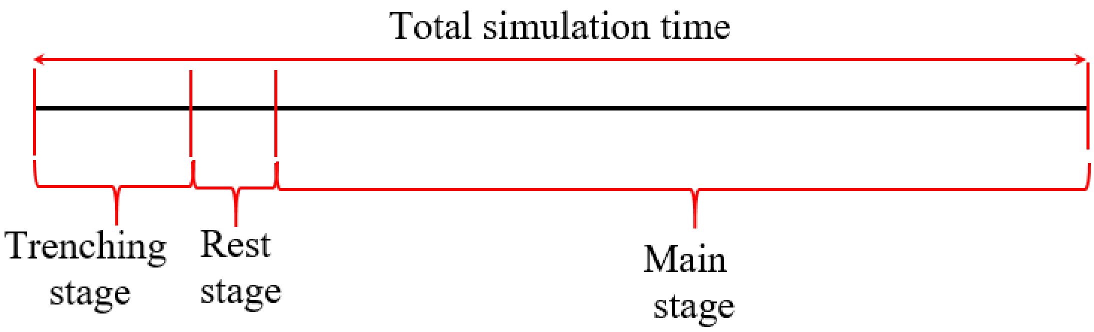

Figure 4 – Simulation stages in the new pre-trenching technique (SSBPT)

1.1.1. Pre-trenching stage

In this stage, the desired pre-trench envelope is created by imposing a suitable trenching wave load on the SCR-vessel system. The vessel response to the trenching load, based on the vessel's response amplitude operators (RAOs) and second-order motions (represented as oscillatory vessel offset in the riser plane), is transferred to the SCR TDZ from the riser top. The SCR TDZ under this motion creates trench progressively. The period for this stage is taken to be the period sufficient to achieve a desired design trench envelope. Hence, several runs may be needed at this stage to decide on suitable pre-trenching load characteristics. The wave loads applied in this stage can be a regular or irregular wave load. However, since many parametric analyses may be needed to determine the suitable load required to create the desired trench envelope, regular wave loads will be ideal for this stage. The RQ model would naturally not provide sufficient depth and span length for trench under normal loading conditions. Hence, the regular trenching load is coupled with the vessel's second-order motion (offsets) to significantly enhance the pre-trench profile creation process.

The vessel RAO is a transfer function that defines the vessel six degrees of motions (6DOM) per unit wave height impact, at a given period, a given wave direction and a given vessel draft. RAOs are usually referenced from the vessel origin, and the resulting vessel motion under wave load conditions are transferred to the riser hang-off by rigid-body motion transfer. Once the RAO for the vessel is set in preparation for the riser analyses (pre-trenching, rest, and main stage) they do not have to be changed during simulation. Hence, the user of the SSBPT may be constrained to use the same vessel RAO for all the stages. In this work, two vessel RAOs are provided, namely the floating production storage and offloading (FPSO) RAO presented in Figure 10 (section 4) used for the major analysis in this work, and the Spar RAO presented in Figure 8 (b), used for the purpose of comparison of the SSBPT technique with existing literature. The oscillatory vessel offsets are the vessel's forced to and fro motion about its nominal position along the riser plane, as depicted in Figure 5. It is used in conjunction with the trenching wave load and the RQ soil model to enhance trench creation by the SCR TDZ. As the vessel undergoes these offsets, the riser hang-off experiences the same offset, causing some offset motions in the TDZ. The vessel offsets in combination with the vessel 6DOM under the pre-trenching wave loads cause the TDZ to trench itself deeper into the seabed more quickly than in scenarios where only the vessel motion is imposed, as will be seen later. The suitable amplitude of the vessel offsets can be expressed in terms of the water depth and is determined from the pre-trench parametric study. In this work, the period of this oscillation is taken to be 100 sec. Note that these oscillatory vessel offsets are used only to enhance the pre-trenching process and must be discontinued during the main stage where the fatigue analysis of the SCR TDZ is conducted. Once a suitable pre-trenching load characteristic (wave loads, vessel offset amplitude and period) have been decided from the pre-trenching parametric study, the load time history on the vessel over the pre- trenching stage is then generated and stored.

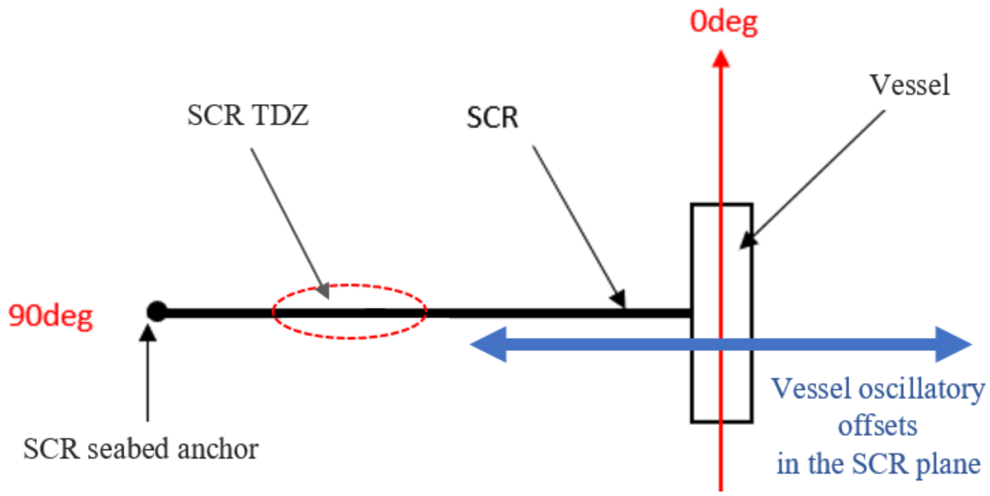

Figure 5 – Induced vessel oscillatory offsets along the riser plane to enhance pre-trenching process

1.1.2. Rest stage

The rest stage is the transition from the pre-trenching stage to the main stage. Transitioning from the pre-trenching to the main stage can result in turbulent responses transmitted to the SCR TDZ that can distort the created pre-trench envelope created at the pre-trenching stage. This can result in a severe distortion of the SCR TDZ fatigue response during the main stage. Hence, there is the need to dampen the pre-trench response and to set the SCR system to its nominal configuration just before the main stage simulation starts. To achieve the dampening process, the time history of the pre-trenching stage is examined, and the simulation times of the peak responses of the last motion cycles of the vessel are obtained. The time at which these peaks occur matches with the zero-velocity point for their motions but may not match when the SCR assumes its nominal configuration. Hence, the vessel needs to be smoothly brought back to its nominal position before starting the main stage simulation. If this process is not conducted smoothly, there is a high tendency that the pre trench already created will be numerically distorted. Therefore, it is important to check the state of the created pre-trench at the end of the rest stage to ensure that its profile is successfully retained into the main stage simulation where it is needed. Exponential, sinusoidal and linear damping functions were tested. Only the linear damping process preserved the pre-trench profile and hence is applied to the rest stage time history. Equation (1) presents the linear model used, where x is the rest stage time history profile (linear) for any of the 6DOF motion, x_1 is the peak value of the response in the last load cycle of the trenching stage, t_1 is the simulation time at which x_1 occur, x_2 is the final response value (the nominal configuration at the start of the main stage), t_2 is the end of the rest stage (coinciding with the start of the main stage). Hence t_2 must be selected long enough to make the slope (velocity) small. In this study, a rest stage $(t_2 - t_1)$ of 600sec was sufficient for all 6DOF. The vessel time history during the rest stage is generated and stored.

$$x = x_1 + \frac{x_2 - x_1}{t_2 - t_1}(t - t_1) \tag{1}$$

1.1.3. The main stage

The main stage is the major stage of interest, where the realistic irregular storm and fatigue wave loads are applied. This stage can be an irregular wave simulation of the riser-vessel system or a simplified simulation of an equivalent regular wave. The wave loads are applied to the vessel, and the resulting vessel 6DOF motions are generated and stored. This pre-trenching technique provides the opportunity to include the second-order vessel motions (or vessel excursions) in this stage. Usually, SCR fatigue simulation is conducted with the vessel in nominal position (no vessel offset). This is conservative since particular sections of the active SCR TDZ maintain longer seabed contact while in nominal position, compared with the case where the vessel's offsets are included during the main stage simulation. The vessel's second-order drift during the main stage will cause the spreading and consequent reduction in the fatigue damage over the longer riser TDZ section, resulting in an overall reduction in the fatigue damage. However, for the demonstrated examples in this work, while the vessel's second-order motion (implemented as oscillatory offsets about the mean vessel position) is included at the pre-trenching stage, it is discontinued at the main stage.

The Rainflow counting technique (Matsuishi and Endo 1968) is applied for the fatigue calculation in this work. The rain flow counting technique expresses the varying SCR stress spectrum as a histogram of stress reversals. The Miner's rule, presented in equation (2), is then applied to cumulate the fatigue damage along the SCR TDZ, where C is the fraction of life consumed by exposure of the riser to cycles of different stress reversals, n_i is the i^{th} stress range amplitude components, N_i is the number of cycles to failure associated with the i^{th} stress range as obtained from the S-N curve. The S-N D-curve in water with cathodic protection (Veritas 2010) is used for the significant analysis. However, in section 3, the-N E- class in seawater is used for the comparative study of the SSBPT with results from the literature

$$C = \sum_i \frac{n_i}{N_i} \tag{2}$$

1.1.4. Composing simulation stage time histories

Once each of the above stages is completed independently, the generated motion time histories from the three stages are then composed to a single load time history as depicted in Figure 4. This single time history is then imposed on the vessel in a single simulation run. The resulting fatigue responses in the SCR TDZ are post-processed in the main stage. The impact of pre-trench conditions can then be evaluated and compared with the no-pre-trench (flat seabed) condition. Note that the trenching stage simulation should be sufficient for the desired pre-trench profile envelope to be created. Simulating the vessel-riser systems under the pre-trenching load beyond the trenching period can result in further incremental or a stabilised trench envelope. The rest stage's simulation time should be sufficient for the riser's transient response to dampen out successfully to avoid distortion of the created pre-trench envelope. The main stage simulation time is the numerical time adequate to achieve considerable confidence in the fatigue results. This depends on the balance between available computation power, result convergencies, and correctness. The main stage simulation period of 7200sec is used in this work.

1.2. Analysis methodology

Figure 4 presents the analysis flowchart for the SSBPT. For the demonstration example in this paper, the OrcaFlex FE software package is used to conduct the numerical computation. Simulations are performed in the time domain, and the implicit integration scheme is applied in the numerical solution process. The modelling, pre-processing, simulations and post-processing are automated using MATLAB programs integrated with the OrcaFlex programming interface, OrcFxAPI (Heffernan 2016). The MATLAB program is used to create the initial OrcaFlex SCR model using the catenary equations. The vessel model, RQ soil model, the selected pre-trenching loads, and the fatigue wave loads are modelled through the MATLAB program as needed, depending on the simulation stage as described by the flow chart in Figure 6. The pre-trenching regular wave load are modelled with the Dean Stream theory, while the irregular wave fatigue loads for the main stage simulation are modelled using the JONSWAP spectrum. The oscillatory vessel offsets about the vessel mean position, representative of the vessel excursions is only imposed on the vessel during the pre-trenching stage. The length of simulation time for each stage are presented in Table 1. The S-N fatigue D-curve in seawater with cathodic protection (AS 2011) is applied for the fatigue damage calculation. Numerical fatigue responses are only post-processed during the main stage, using the Rain flow counting technique (Matsuishi and Endo 1968).

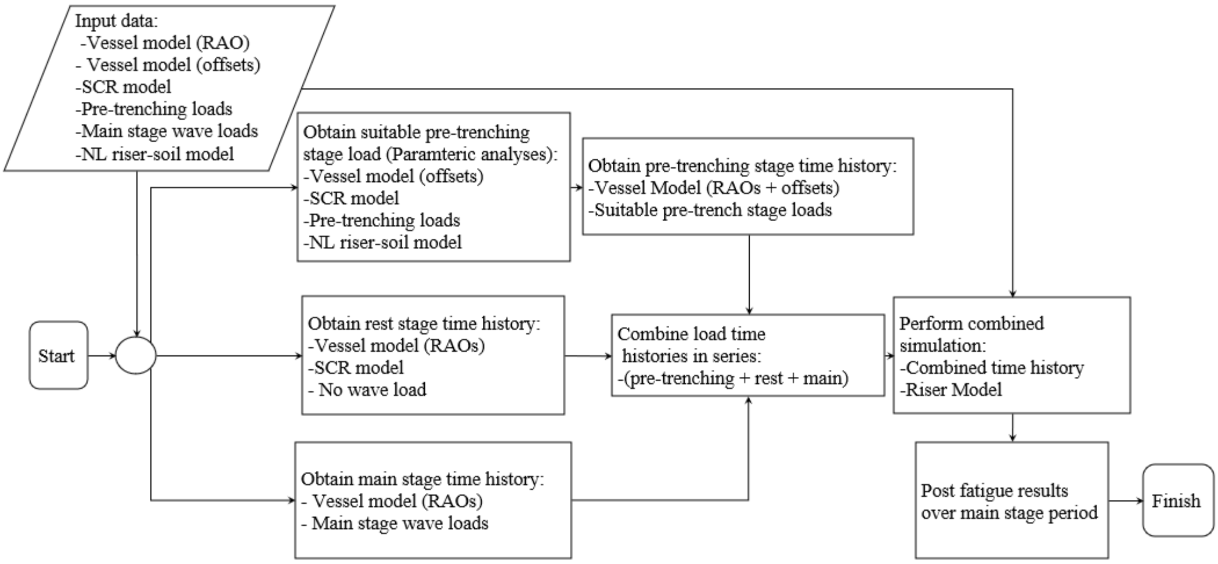

Figure 6 – Analysis flowchart

Table 1 –Simulation stages and associated time lengths

Analysis steps	**Simulation time (sec)**
Trenching Stage	1000
Rest Stage	600
Main Stage	7200
Single run (combined time history)	8800

Comparing the SSBPT with existing literature

The simulation stage-based pre-trenching technique (SSBPT) is developed based on the potentials of the hysteretic non-linear SCR soil interaction model (RQ model)(Randolph and Quiggin 2009). It is expedient to compare the capability of this technique to other techniques developed on the same model (like for like comparison). The study with which the SSBPT is compared is available in (Shoghi and Shiri 2019). In that work, the authors conducted qualitative comparisons of fatigue damage response of the SCR TDZ in three different mathematical adjusted trench profiles presented in Figure 7. These are the linear-exponential trench, the quadratic-exponential trench obtained from (Shiri 2014a), and a polynomial trench obtained from (Langner 2003). The technique uses the RQ model in OrcaFlex but with adjusted values of the penetration factor and suction ratio to create initial numerical trenches. The adjusted soil data are then reset to their nominal values once the desired pre-trench has been made. These created trench profiles are modified based on the aforementioned mathematical profiles and then modelled through a specially developed in-house routine in Abacus for the fatigue simulation. These processes are understandable since, in OrcaFlex, the restart facility does not provide the capability for resetting the RQ model data in a single fatigue simulation run once the simulation is initiated. Hence, it is not yet directly possible to create these trenches and conduct the fatigue damage analysis in the same process unless an incremental trenching process is considered (no soil data modification), which is the default no pre-trench scenario. Also, the resulting trenches developed by the authors' technique may not provide a sufficiently longer span typical with observed field data. This may have necessitated further modifications of similar trenches through the stepped trench profile technique developed by Mekha, Randolph, Bhat and Jain 2013 (see Figure 3). However, the SSBPT technique uses the actual soil data, but with a large regular wave, vessel motions, and oscillatory vessel offsets in a single simulation run, without the need for external modification of the numerical trenches or its data. The technique takes advantage of other powerful features that OrcaFlex provide in handling such non-linear interactions for the penetrating SCR TDZ under complex loading in the presence of the created pre-trench.

The SSBPT pre-trench parametric study is conducted in search of trench profiles that have similar depth as the three profiles from Shoghi and Shiri 2019. Regular wave loads with height ranging from 1m to 10m, with corresponding periods around the spar peak heave period (23sec to 35sec) (see Figure 8 (b)), and vessel oscillatory offset of 0%, 2%, 6%, 8% and 10% of the water depth were applied for this purpose. The pre-trenching process was conducted over a period of 1000sec with an oscillatory vessel offset period of 100sec. Among the pre-trenches created and investigated, attention is drawn to two pre-trench envelopes that are similar in depths to those used by Shoghi and Shiri 2019. These two pre-trenches are included in Figure 7 and are created using the following pre-trenching load:

- SSBPT Trench1: pre-trench envelope created from H = 19m, T = 32sec, vessel offset = 2%
- SSBPT Trench2: pre-trench envelope created from H = 20m, T = 31sec, vessel offset = 0%

The general data obtained from (Shoghi and Shiri 2019) used for the fatigue analysis are summarised in Table 2. The joint fatigue wave data, the spar vessel RAO and the RQ model data used are presented in Figure 8 (a), (b) and (c), respectively. Note that these data are only used to obtain results with the SSBPT for comparison purposes. The data applied for the main investigation in this paper are presented in section 4.

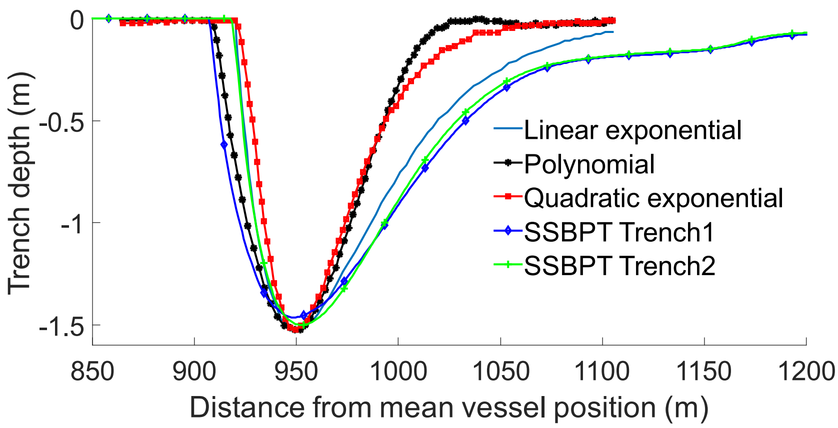

Figure 7. Pre-trench envelopes for comparison purposes

Table 2 – Analysis data used for the comparative analysis

Data	**Values**
SCR pipe outer diameter - OD	0.324 m
SCR in service weight	100 kg/m
Pipe bending stiffness	4.67E7 N.m^2
SCR total length	2333 m
Hydrodynamic coefficients $[C_d, C_M, C_a]$	[0.7,1.5,1.0]
SCR nominal TDP from vessel hull centre	949.4 m
SCR seabed anchor from hull centre	1306.6 m
SCR hang off-angle (with vertical)	12 °
SCR hanging length	1975.8m
Fatigue S-N curve $[m_1, log\bar{a}_1, log\bar{a}_2]$	E-class in seawater (AS 2011)
Fatigue wave data $[H_s(\text{m}), T_z(\text{sec}), N]$	See wave table in Figure 8 (a)
Pre-trench depth (4.63OD)	1.5 m
Water depth	1600 m
Spar COG below MSL	110 m
SCR connection to hull below COG	90 m

(a)

S/N	Hs	Tz	Cycles	S/N	Hs	Tz	Cycles
1	0.5	4.2	18011291	16	8	9.1	3389
2	1	4.6	71370445	17	8.5	9.3	3011
3	1.5	5	48449608	18	9	9.5	1822
4	2	5.4	25187856	19	9.5	9.7	1395
5	2.5	5.8	13529335	20	10	9.9	1070
6	3	6.1	7473660	21	10.5	10.1	1246
7	3.5	6.5	3080495	22	11	10.2	566
8	4	6.9	1631014	23	11.5	10.4	928
9	4.5	7.3	583770	24	12	10.6	544
10	5	7.7	363725	25	12.5	10.7	813
11	5.5	8	114700	26	13	10.9	712
12	6	8.4	33676	27	13.5	11	877
13	6.5	8.5	16907	28	14	11.2	262
14	7	8.7	10864	29	14.5	11.3	343
15	7.5	8.9	5421	30	15	11.5	420

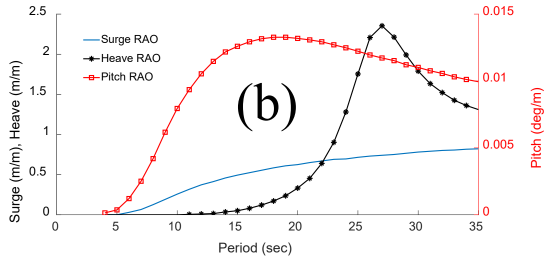

(c)

Parameter	Symbol	Value
Mudline shear strength	s_{u0}	0.65 kPa
Shear strength gradient	ρ	1.5 kPa/m
Power law parameter	a	6
Power law parameter	b	0.25
Normalized maximum stiffness	K_{max}	200
Suction ratio	f_{suc}	0.3
Suction decay parameter	λ_{suc}	0.5
Repenetration parameter	λ_{rep}	0.5

Figure 8. (a) Fatigue wave data; (b) Spar vessel response amplitude operators (RAO); (c) NL hysteretic soil interaction model (RQ model) data.

The fatigue analyses are conducted for the SCR for the pre-trench-2 condition as the riser is exposed to the 30 wave loads presented in Figure 8 (a). The joint fatigues damage response is obtained from the main simulation stage of the SSBPT, to be compared with the results based on the three pre-trench envelopes from (Shoghi and Shiri 2019). It is noteworthy here that authors of the validating literature (Shoghi and Shiri 2019) have indicated that their results are intended for qualitative purposes rather than quantitative assessments. A qualitative comparison of the fatigue damage results from the validating literature and the SSBPT are presented in Figure 9. For this comparison, the fatigue damages from the pre-trenched cases in the respective studies are normalised by the maximum fatigue damage from the flat seabed or no pre-trench case. In general, the pre-trench fatigue damage is greater than the flat seabed cases, as is in the validating results. Although the fatigue damage peaks occur around the same arc length, the SSBPT technique provides greater fatigue damage on SCR TDZ sections neighbouring the peak damage arc length. This makes some sense since the 30 wave loads applied have a wide range of significant wave heights and zero up crossing periods, and the impact of these waves on the vessel may result in a more spreaded fatigue damage within the SCR TDZ. Also, the SCR TDZ sections beyond the trench surface points are expected to incur some level of damage from these combined wave loads excitations. It is expected that as the excitation in the SCR dampens out towards the SCR seabed anchor, the fatigue damage along it will reduce accordingly as observed from the SSBPT result. The authors would like to summarise at this point that this comparison is by no means a conclusion on whether the pre-trench induces greater fatigue damage or not as that will depend on a wider range of variables, which we believe the SSBPT provide opportunities to model and to investigate.

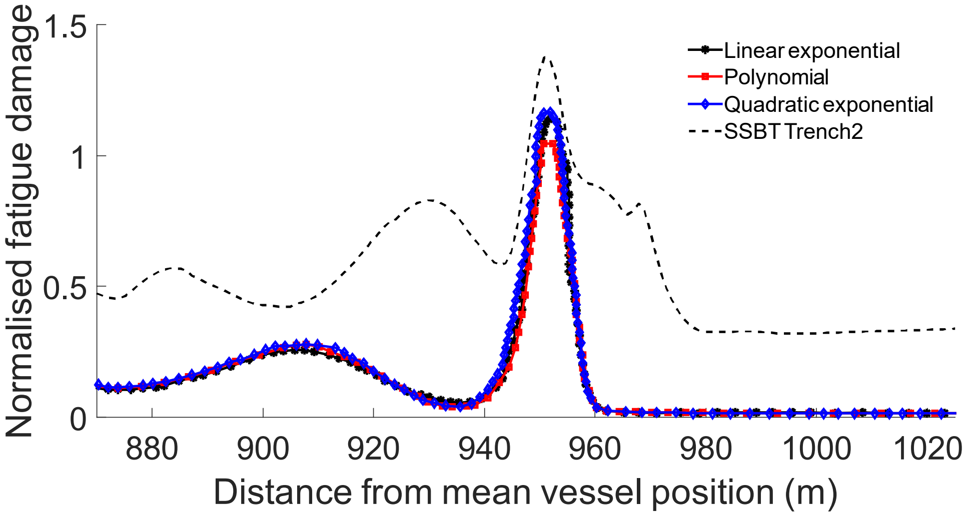

Figure 9. Normalised fatigue damage response of the SCR for the validating literature and the SSBPT.

2. Main Analysis Data

The general analysis data for the main investigation in this paper is presented in Figure 4. Three pre-trench conditions are considered in this investigation. They are the no-pre trench (flat seabed), pre-trench-1 of depth 2.04OD and pre-trench-2 of depth 4.49OD. The significance of selecting these three pre-trench conditions in this study is to demonstrate the different SCR TDZ fatigue damage responses in the different scenarios of pre-trench conditions. Further justification for selecting these pre-trench conditions is discussed in Section 5.2. Note that 1OD = 0.232m as presented in Figure 4. The SCR pipe considered for this study is a bare steel pipe with no insulation and internal coating layers. The insulation layers (if included) is usually not considered stress-bearing layers for the SCR. For the interaction of the riser TDZ with the seabed, the stiffness provided by the riser pipe is taken to be the axial stiffness, EA_s, and bending stiffness, EI of the steel layer, where E is the young's modulus, A_s is the steel pipe cross sectional area (single wall steel pipe in this case), and I is the second moment of area of the SCR pipe.

For the main stage, the simulated fatigue wave loads are presented in Table 4. The wave loads are applied to the vessel-riser system in the riser azimuth direction, which happens to be beam waves for the vessel. This wave load direction is set to induce maximum vessel roll and heave, which impact high motions on the SCR TDZ. The five-wave loads from Table 4 and the three pre-trenching conditions are combined to derive fifteen analysis cases presented in Table 7 of section 5.3.

The nonlinear hysteretic SCR-seabed interaction model (RQ model) is used in this study. The seabed model possesses the capability for incremental seabed trenching, which is employed in the SSBPT to create longer and deeper pre-trenches under high SCR excitations. The RQ model penetration modes and characteristics were presented in Figure 2. Details of the RQ model can be found in (Randolph and Quiggin 2009). The default soil parameters for the RQ model for clay soil is used in this study and are presented in

Table 5.

Table 3 – Main analysis data

Data	Values
SCR pipe outer diameter - OD	0.2032 m
Wall thickness (single wall)	0.0183 mm
In service weight	63.3 kg/m
Young modulus of pipe material (E)	2.12E+08 kPa
Axial and bending stiffness (EA_s)	2.3E6 kN
Bending stiffness (EI)	9.7E3 kN.m^2
Hydrodynamic coefficients $[C_d, C_M, C_a]$	[0.7,2.0,1.0]
SCR content density	600kg/m^3
SCR content pressure	10 ksi

SCR hang off with the vertical	12 °
Nominal height of SCR (Water depth)	1500m
Fatigue S-N curve (with cathodic protection)	D-class in seawater (Veritas 2010)
Fatigue wave data [H_s(m), T_z (sec), N]	See Table 4
Pre-trench depths (OD)	No trench≈ 0OD, trench1≈ $2OD$, trench2≈ $4.5OD$
FPSO RAOs (Heave and roll responses)	See Figure 10
FPSO RAOs symmetry (see Figure 1)	The longitudinal and transverse axes
SCR connection to FPSO hull	Mean sea level, transverse axis

The most relevant vessel RAOs, considering the direction of wave load application, are presented in Figure 10

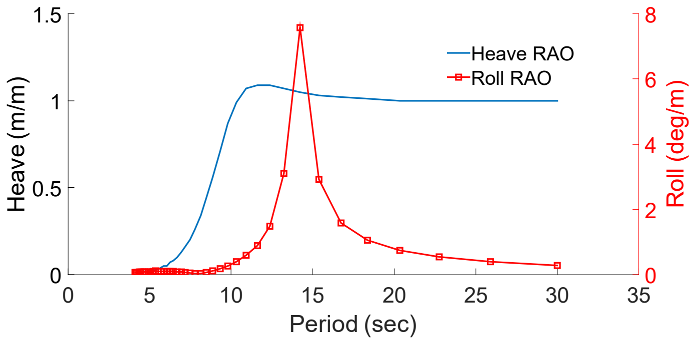

Figure 10. FPSO response amplitude operators (RAO).

Table 4 –Fatigue wave data to be applied during the main stage

Wave No	**Irregular wave loads**		
	Hs (m)	**Tp (sec)**	γ
1	1.5	5.5	1.8
2	3	8.8	1.0
3	4.5	9.5	1.6
4	8	13	1.6
5	15.8	16.9	2.4

Table 5 – The nominal hysteretic non-linear soil data (Randolph and Quiggin 2009)

Data	**Units**	**Values.**
Soil model parameters:		
Penetration resistance parameters (a, b)	-	(6.00, 0.25)
Soil Buoyancy factor (f_b)	-	0.25
Normalised maximum stiffness (K_{max})	-	1.50
Shear strength at mudline	kPa	5.0
Shear strength gradient	kPa/m	1.5
Saturated soil density	te/m^3	1.5
Suction resistance ratio (f_{suc})	-	200.00
Normalised suction decay distance (γ_{suc})	-	0.60
Normalised re-penetration offsets after uplift (λ_{rep})	-	0.3

Main Analysis, Results and Discussions

In the result presentation of the trench profile and the SCR response, the abscissa is presented in arc lengths of the SCR, which is its length from the hang-off point. Please, note that each point along the trench profile uniquely matched each point along the SCR TDZ which created it i.e., each point along the trench profile represents the penetration of a unique point on the SCR TDZ. This nomenclature will help to make a one-to-one comparison of the trench depth of a point along the trench profile with the fatigue response of the corresponding point on the SCR TDZ.

2.1. Pre-trenching parametric analysis

The selection process of an appropriate regular wave load to create a desired design pre-trench envelope requires a parametric study. Regular wave loads ranging from 1m to 10 m, with corresponding periods above their breaking wave limit, are simulated up to 1000 sec. The regular trenching wave load table investigated is presented in Table 6

Table 6 – Regular wave load for pre-trenching parametric study

H (m)	**T (sec)**									
1	3	5	7	9	11	13	15	17	19	21
2	4	6	8	10	12	14	16	18	20	22
3	4	6	8	10	12	14	16	18	20	22
4	5	7	9	11	13	15	17	19	21	23
5	5	7	9	11	13	15	17	19	21	23
6	6	8	10	12	14	16	18	20	22	24
7	6	8	10	12	14	16	18	20	22	24
8	7	9	11	13	15	17	19	21	23	25
9	7	9	11	13	15	17	19	21	23	25
10	7	9	11	13	15	17	19	21	23	25

The wave-table is simulated along with oscillatory vessel offsets of 2%, 4%, 6% and 8% water depth. 400 pre-trenched envelop were examined, but a few of the resulting trench profile envelopes are presented in Figure 11 to Figure 13 to describe some peculiar features.

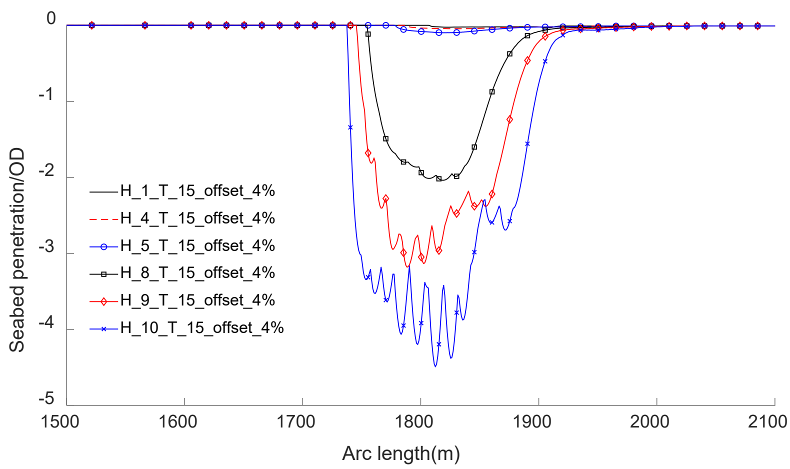

Figure 11 –Pre-trench profile envelopes for increasing trenching load amplitude with 4% vessel oscillatory offsets

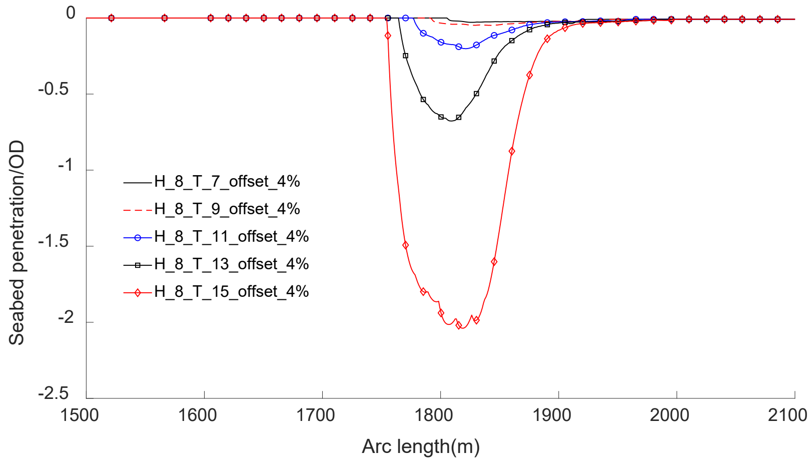

Figure 12 – Pre-trench profile envelopes for increasing trenching load period with 4% vessel oscillatory offsets

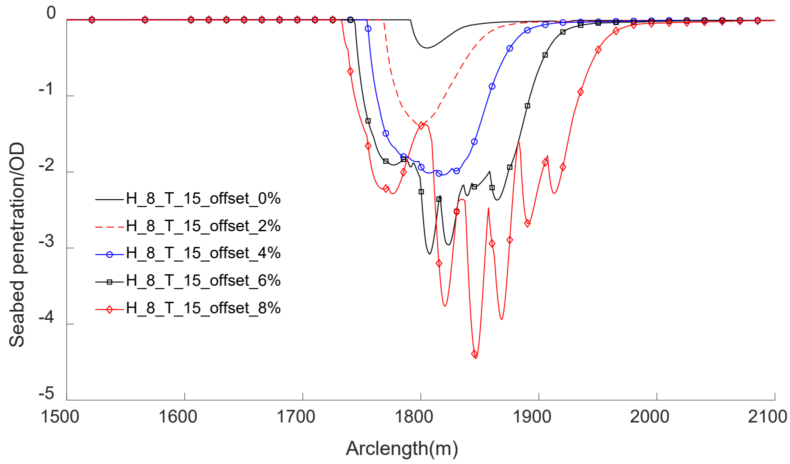

Figure 13 – Pre-trench profile envelopes for increasing oscillatory vessel offset

The following are observed for the pre-trench profile envelope in Figure 11 to Figure 13

1. The pre-trench envelopes, characterised by their depths and lengths, expands and deepens with increasing regular trenching load amplitude, as seen in Figure 11. However, it can be observed that higher values of H result in a more irregular trench profile pattern. This may be attributed to the combined response of the seabed and the riser under the trenching load. If the riser TDZ is infinitely stiff globally, higher trenching load amplitude will result in deeper and smoother pre-trench envelope boundaries. However, because the riser TDZ is globally deformable, its shape can rapidly deform under higher load amplitude in the presence of the seabed resistance, resulting in rougher pre-trench envelop boundaries.

2. The pre-trench envelopes expand with increasing regular trenching load period, as seen in Figure 12. It can be observed that periods between 13sec and 15sec provide deeper and longer span pre-trench envelopes. This could be because the joint vessel heave and roll responses are more significant within this range, as shown in Figure 10. Similar observations were also made for the pre-trenching parametric study for the comparative analysis in section 3. It should be noted that the trenching stage is the stage where the designed trench profile is created, and no fatigue damage responses should be post-processed from it. Fatigue damage response should only be post-processed from the main stage where the system's actual fatigue wave load is applied. Hence, we can take advantage of the resonance period of the vessel excitations to enhance the pre-trench creation process.

3. The pre-trench envelopes expand with increasing oscillatory vessel offsets, as seen in Figure 13. It can be observed that for larger vessel oscillatory offsets (e.g. 10% of the water depth), the trench profile envelope starts to become irregular. This behaviour may be associated with the large range in the change of the SCR TDZ curvatures due to larger vessel offsets. Such large-amplitude vessel offsets are only mentioned here to understand the created pre-trench profiles under them but are not practicable considering fatigue loading conditions.

2.2. Selected pre-trenching conditions for fatigue analysis

Figure 13 shows that the trench-envelope created in the vessel offset condition and that created in the no-vessel offset conditions are significantly different. This indicates that the vessel offsets or excursions during SCR installation and operations may substantially impact the trench evolution process as numerically observed during the pre-trenching parametric analysis. The three pre-trenched conditions presented in Figure 14 are those selected for this study, derived from the trench parametric analyses conducted in section 0. According to Table 7, these three selected pre-trench conditions for which the five fatigue wave loads (see Table 4) will be investigated were created with the following pre-trenching excitation conditions at the pre-trenching stage.

- No pre-trench (flat seabed): H = NA, T = NA, oscillatory vessel offset amplitude = NA
- Pre-trench 1: H = 8m, T = 15sec, oscillatory vessel offset amplitude = 4%
- Pre-trench 2: H = 10m, T = 15sec, oscillatory vessel offsets amplitude = 4%

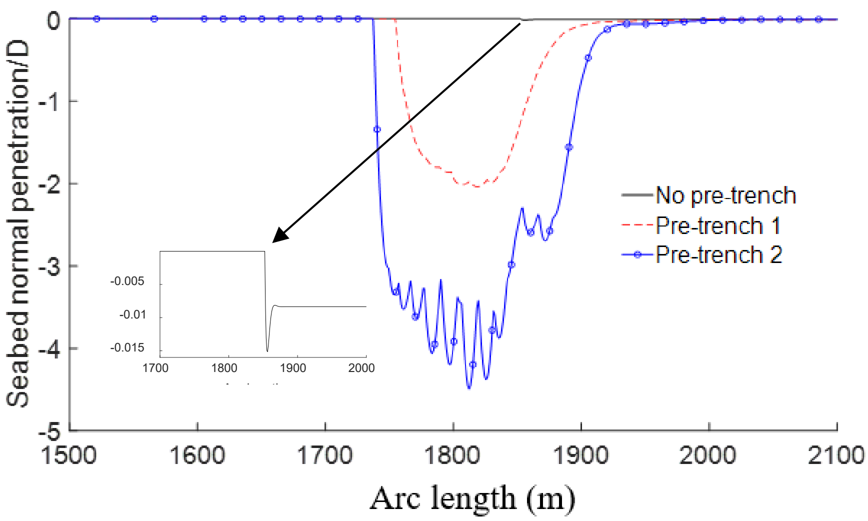

Figure 14 – Pre-trench profile envelope selected for fatigue analysis

The justifications for the selected three pre-trench conditions are discussed as follows:

- No pre-trench condition: The "No pre-trench" condition represents a "flat seabed" at the beginning of the main stage simulation. This is usually the case for fatigue analysis with the NL SCR-soil interaction model when no pre-trench conditions are considered. The initial trench depth for the flat seabed case is negligible, based on the RQ model. The depth corresponds with the static SCR TDZ penetration, which is about 0.015$\boldsymbol{OD}$ in this study, as seen in Figure 14. Under fatigue loading, the SCR TDZ incrementally creates a trench from the flat seabed and embeds itself into it. There is a need to include this case in the analysis for comparison purposes with the cases where an initial trench is imposed at the beginning of the main stage simulation.

- Moderate pre-trench envelope: When moderate pre-trenches are subject to large SCR TDZ excitation, their trench envelopes are exceeded, and a deeper and stabilised trench will be created within a short time under such high riser motion conditions (Mekha, Randolph, Bhat and Jain 2013). As observed from field data (Bridge and Howells 2007), a trench in trench scenario may also result. It is relevant to have such pre-trench depth to understand how the SCR TDZ fatigue damage behaves when the pre-trench envelope is exceeded. This pre-trench envelope of ≈2OD deep is considered to model and investigate this scenario.

- Deeper pre-trench envelope: Since it is believed that the existing trench created during the riser installation and other environmental influences should be large enough to contain all SCR TDZ motions (Shoghi and Shiri 2020), this relatively deeper trench of $\approx 4\boldsymbol{OD}$ is considered. For this pre-trench conditions, the pre-trench envelope is large enough to contain the motions of the SCR TDZ under moderate SCR excitations typical of fatigue load.

2.3. Load case table and vessel time history for fatigue analysis

Based on the five fatigue wave load data in Table 4 and the selected three pre-trench conditions, the created analysis cases are detailed in Table 7. There will be fifteen groups of 6DOF motion time histories composed from the three stages (see Figure 4). Only two groups of the composed vessel 6DOF time histories are presented in Figure 15 and Figure 16 to provide a visual sense of what they will look like. These are the time histories for case3 and case8, respectively. Note that in the numerical model built for this study, the X-DOF vessel motion is centred about the nominal position (X = 34 m). The X-DOF for case8 in Figure 16 appears to be constant at 34m after the pre-trenching stage. In contrast, it is not, as the vessel oscillations about the X = 34m are negligible compared with the large offsets during the pre-trenching stage (see a different plot scale for case3 in Figure 15. The linear motion dampening for all 6DOF through the resting stage can be seen in Figure 16.

Table 7 – Load case table for the analyses. Note the case numbers (1-15) as referenced in the results discussion section.

Pre-trench conditions + Fatigue wave loads		
No pre-trench	Pre-trench 1	Pre-trench 2
Case No: 1	Case No: 6	Case No:11
Pre-trench = Static (0.015OD)	Pre-trench = 2.04OD	Pre-trench =4.49OD
Pre-trench load:	Pre-trench load:	Pre-trench load:
- H = NA	- H = 8m	- H = 10m
- T = NA	- T = 15sec	- T = 15sec
- Offset = NA	- Offset = 4%	- Offset = 4%
Fatigue wave loads (main stage):	Fatigue wave loads (main stage):	Fatigue wave loads (main stage):
- Case No 1: Plus Wave1	- Case No 6: Plus Wave1	- Case No 11: Plus Wave1
- Case No 2: Plus Wave2	- Case No 7: Plus Wave2	- Case No 12: Plus Wave2
- Case No 3: Plus Wave3	- Case No 8: Plus Wave3	- Case No 13: Plus Wave3
- Case No 4: Plus Wave4	- Case No 9: Plus Wave4	- Case No 14: Plus Wave4
- Case No 5: Plus Wave5	- Case No 10: Plus Wave5	- Case No1 5: Plus Wave5

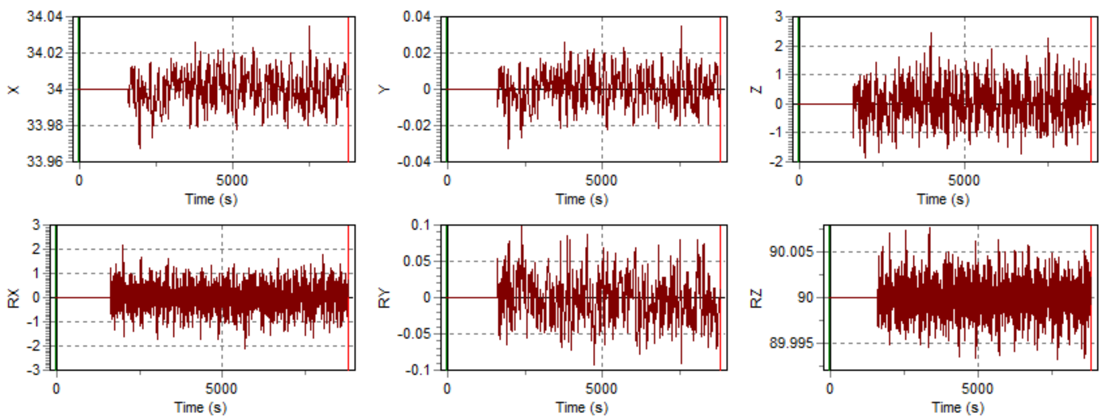

Figure 15 – 6DOF motion time history for case3 in Table 7 (ordinate axes are in metres)

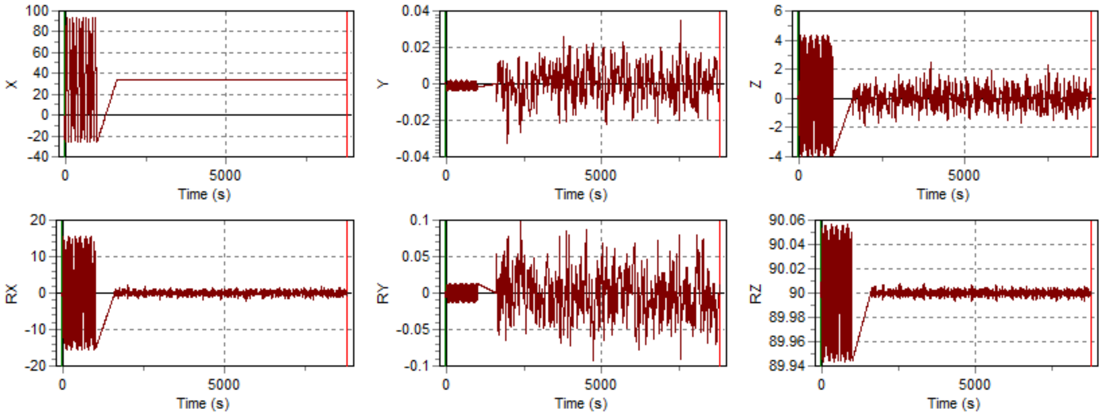

Figure 16 – 6DOF motion time history for case8 in Table 7 (ordinate axes are in metres)

2.4. Pre-trench envelope integrity verification

Refer to Table 1, the main stage simulation starts at (1000sec + 600sec = 1600sec) and ends at 8800sec, which is the sum of the time in all the three simulation stages. First, it is essential to verify that the integrity (profile shape) of the pre-trench envelope created in the pre-trenching stage is preserved by proper dampening out of the trenching loads in the rest stage. To verify this, we present the pre-trench envelopes present at the beginning of the main stage (at 1600sec) for the no pre-trench, the pre-trench1 and the pre-trench2 cases in Figure 17 (a), (b) and (c), respectively. The trench envelopes for all the cases match those presented in Figure 14. This verifies that the desired pre-trench envelope conditions created at the pre-trench stage are available or 'remembered' at the beginning of the main stage for fatigue calculations. This is also an indication that the rest stage linear motion dampening of the vessel 6DOF was effective.

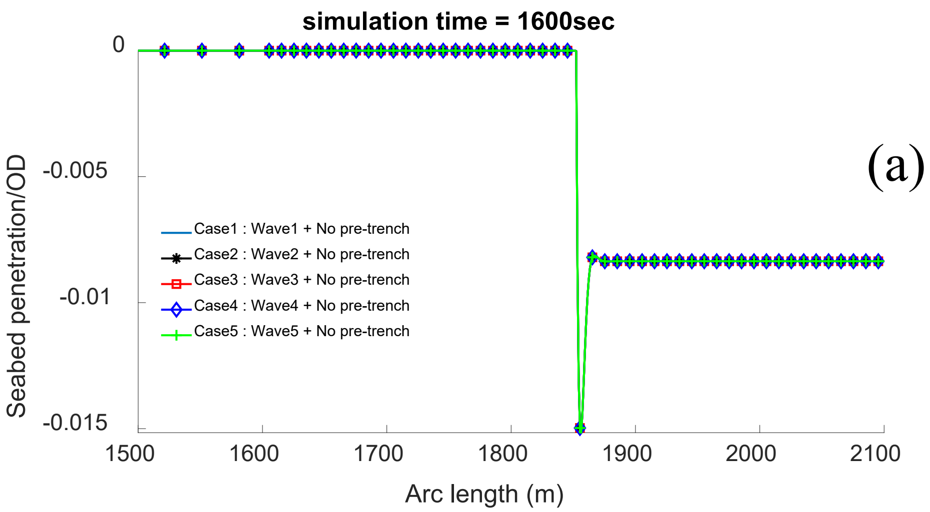

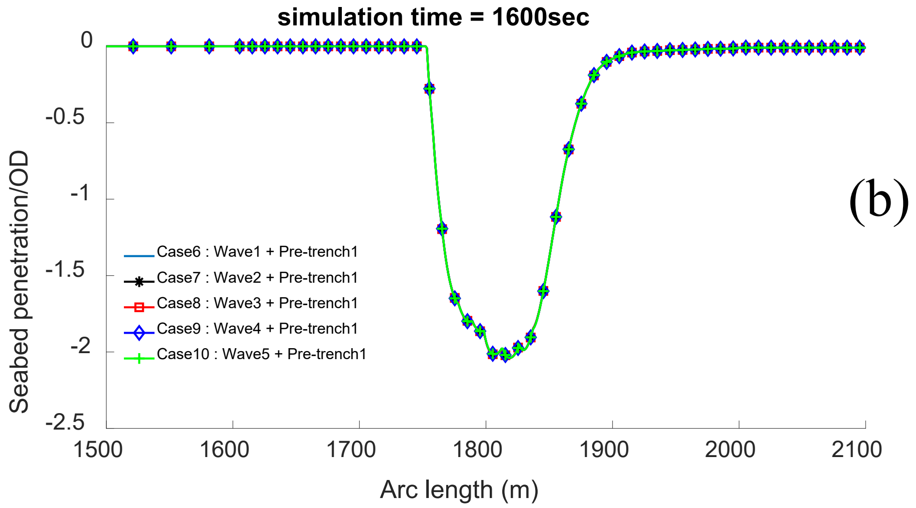

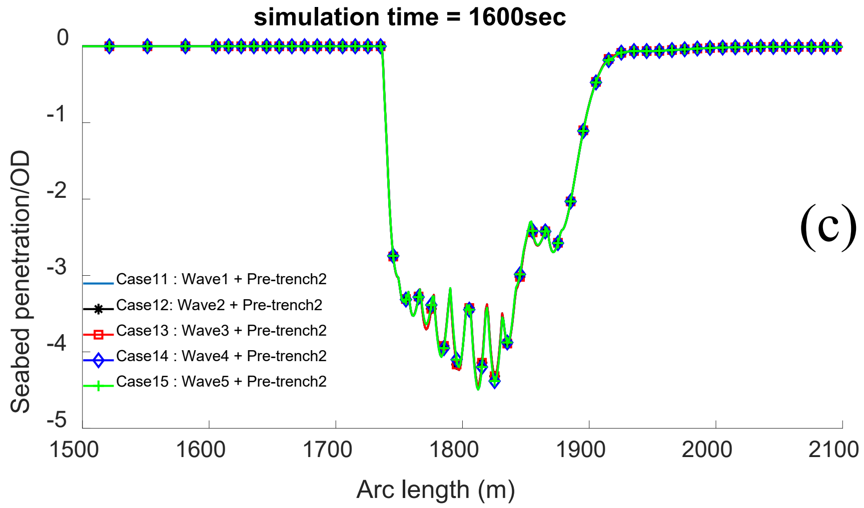

Figure 17 – Pre-trench conditions at the beginning of the main stage simulation for (a) No pre-trench envelope: case1 to case5, (b) Pre-trench1 envelope: case6 to case10, (c) Pre-trench2 envelope: case11 to case15

2.5. Pre-trench envelope and final trench profile

It is important at this point to distinguish between the pre-trench envelope and the final trench profile developed at the end of the main stage simulation. The pre-trench envelope is the trench introduced prior to the main stage simulation, effected in this study using suitable regular wave loads, the vessel motion (RAOs) and the vessel's oscillatory offsets. It can also be referred to as the design trench condition. On the other hand, the final trench is the range graph maximum of the profile created by the SCR TDZ while undergoing motions within the pre-trench envelope during the main stage. The main stage motions are caused only by the fatigue wave load applied to the vessel, defined by the vessel's RAOs. In this study, the vessel 6DOF motion during the main stage is about its mean (nominal) position, i.e., no second-order drift effect is included.

Consider the no pre-trench cases during the main stage, continuous motions of the SCR TDZ cause incremental embedment into the virgin soil until the trench is stabilised at the final trench profile. The final trench profiles for the no pre-trench cases at the end of the main stage are plotted in Figure 18 (a). Recall that the pre-trench envelope for these cases is the static penetration of the riser into the soil ($0.015OD$), which is negligible. It could be observed that as the wave loads increase (implying higher motion amplitude of the SCR TDZ), deeper final trench profiles are created at the end of the main stage, as seen in Figure 18 (a). For example, it is observed in Figure 18 (a) that penetration into the virgin seabed can reach a depth up to 8 times the riser pipe diameter (OD) for wave5 (H = 15.8m, Tp = 16.9sec).

For the pre-trench cases, continuous embedment of the excited SCR TDZ is also experienced but into an already penetrated or softened soil defined by the pre-trench envelope. The SCR TDZ will continue to embed itself deeper into or beyond the pre-trench envelope until the trench profile created stabilises under the applied fatigue load. The final stabilised trench profile in these cases can be less than the pre-trench envelop for cases with relatively lower wave load or motion amplitude (case6, case7, case8 in Figure 18 (b) and case11, case12, case13 in Figure 18(c)). The final trench may also have some of its profile section shallower or deeper than the pre-trench envelop as observed for case9 in Figure 18(b) and case14 in Figure 18(c). Lastly, the final stabilised trench envelope can exceed the pre-trench envelope under high motion amplitudes, as seen for case10 in Figure 18(b) and case15 in Figure 18(c). Therefore, it should be noted that an existing pre-trench envelope can be exceeded if the riser TDZ are excited so much that they penetrate deeper and wider beyond an existing trench wall. The RQ model, which provides the capability for these trenching processes, is developed on the backbone curve, which offers large stiffness resistance to the pipe penetration at the beginning of the loading cycle. This high soil resistance to SCR TDZ penetration is defined by the ultimate penetration resistance curve in Figure 2(b). Hence, small vessel excitations, such as those caused by smaller waves 1,2,3, as observed in Figure 18 (a), (b) and (c), can only result in negligible SCR TDZ penetration. However, once large-amplitude SCR excitations caused by larger waves overcome this high resistance in its first penetration, subsequent soil resistance, defined by the re-penetrations curves, provide less soil resistance and deeper trenches.

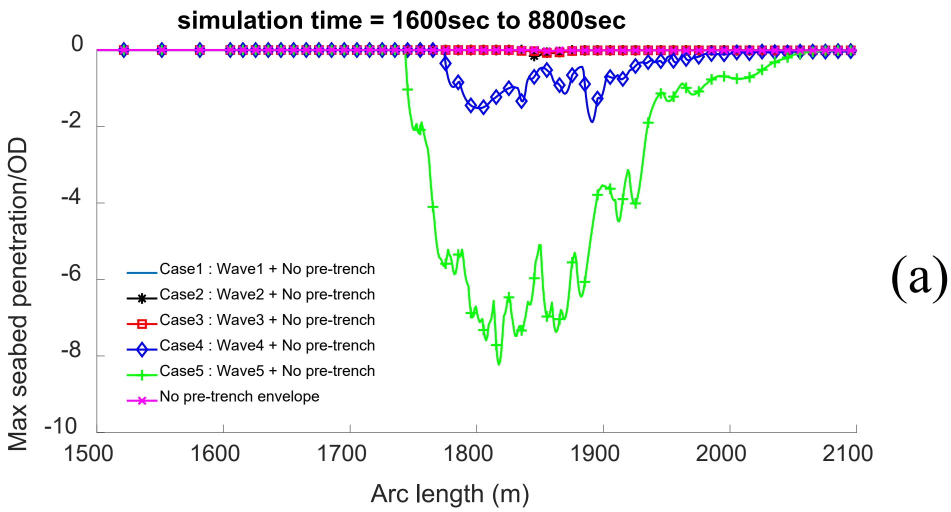

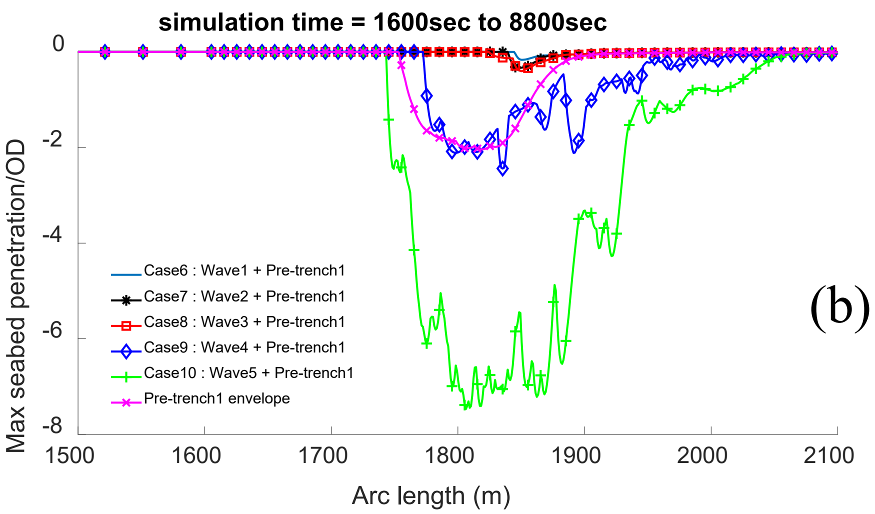

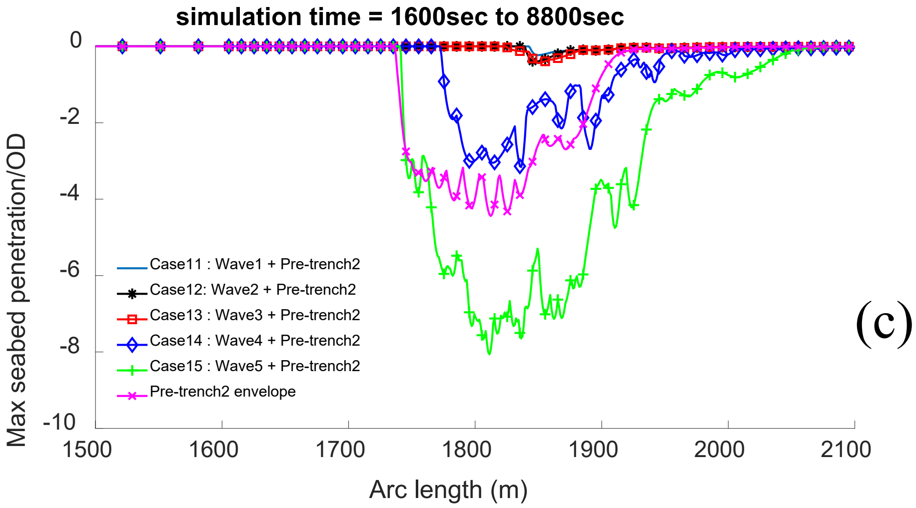

Figure 18 – Final trench profile for pre-trenched cases – (a) No pre-trench (b) pre-trench1 (c) pre-trench2, at the end of the main stage

2.6. Investigating pre-trench envelope impact on SCR TDZ fatigue damage response

To investigate the impact of pre-trench on the fatigue damage response of the SCR TDZ. Each of the five fatigue wave loads (Wave1, Wave2, Wave3, Wave4 and Wave5) is applied across the three pre-trench conditions (No pre-trench, pre-trench1, and pre-trench2). The final trench profile and the corresponding fatigue damage responses of the SCR TDZ are presented in Figure 19 to Figure 23. A summary of the fatigue damage response is presented in Table 8. Figure 24 presents the percentage increase or decrease of the SCR TDZ fatigue damage response for the pre-trench cases relative to the no pre-trench cases.

Generally, it could be observed from the results that irrespective of the presence of a pre-trench or no pre-trench conditions, SCR fatigue damage increases with increasing applied wave load. As the pre-trench envelop gets deeper, and the fatigue wave load amplitude increases, the fatigue damage incurred by the SCR TDZ increases, as long as the motion of the SCR TDZ does not result in a final trench profile that is equal to or exceeds the pre-trench envelope. The increasing trend can be seen for wave1, wave2 and wave3 cases in Figure 19(b), Figure 20(b), Figure 21(b), the first three result rows of Table 8 and Figure 24. Also, see Figure 18(b) and Figure 18(c) to compare the final trench profile caused by wave1,wave2 and wave3 relative to the pre-trench1 and pre-trench2 envelope. For example, it could be seen from Figure 24 that wave3 + pre- trench1 (case8) and wave3 + pre-trench2 (case13) resulted in up to 60% and 70% increase in fatigue damage compared with their respective no pre-trench cases. As the wave load amplitudes decrease from wave3 through wave2 to wave1, increase fatigue damage relative to respective no pre-trench cases are observed (for both pre-trench1 and pre-trench2) but in decreasing order of the wave amplitudes as seen in Figure 24.

When the final trench profile matches or exceeds the pre-trench envelope, irrespective of the wave load amplitude in action, there will be less difference between the SCR fatigue response in the pre-trenched case and the no pre-trench case. This can be seen for wave4 and wave5 for pre-trench1 and pre-trench2 conditions in Figure 22(b), Figure 23 (b), and Figure 24. For example, consider a high sea state condition typical of the North Sea. If the existing pre-trench caused by extreme events cannot accommodate the SCR TDZ motions under the fatigue load, further trenching beyond the pre-trench envelop results and the corresponding fatigue damage of the pre-trench case will be of equal magnitude as that of the no pre-trench condition. This may also be true for low sea states plus an existing smaller pre-trench that can be exceeded by the SCR motions caused by the low sea conditions. This indicates that the relevance of pre-trench or no pre-trench in the design analysis of SCRs should be a joint consideration of the available design trench envelope and the motion amplitudes of the SCR TDZ caused by the wave loads and the vessel RAOs.

When the applied wave loads result in SCR TDZ motion amplitudes that are just contained within or exceed the pre-trench envelope, the SCR TDZ nodes will interact closely with some or all parts of the pre-trench envelop boundaries over the loading cycles. This was observed for the Wave4, which created final trench profiles that are either shallower or deeper than parts of the boundaries of the pre-trench envelope, as seen in Figure 18(b) and Figure 18(c). There will be regular pressure hot spots created between the pre-trench envelope boundaries and the SCR TDZ nodes for such wave conditions and design pre-trench envelope. These hotspots are not artificial in this case since the pre-trench envelope wall is not constrained to a fixed envelope (as done in most studies) but allowed to be trenched through by higher amplitude SCR TDZ. Hence, these are natural SCR TDZ interactions with trench walls as captured by the SSBPT. Such a combination of wave load and pre-trench condition results in a random trenching response of the SCR TDZ, as seen in the final trench profile in Figure 22(a). For cases like this, it is not obvious whether the pre-trench cases induce greater fatigue damage than the no pre-trench cases. In fact, as can be seen in Figure 22 (b), the pre-trench conditions and the no pre-trench conditions induces greater fatigue damages than the other at different sections of the SCR TDZ. However, the difference in peak fatigue damage between the trenched and the no trenched conditions for this type of combined wave load and pre-trench conditions is small, even with the higher amplitude wave5 as observed in Figure 24. It could be seen from Figure 24 that while pre-trench1 resulted in about a 3.7% decrease in fatigue damage, pre-trench2 resulted in about a 2.3% increase in the fatigue damage compared with the no pre-trench case for wave5. Hence, the fatigue damage patterns for these conditions are difficult to predict.

Consider a calm sea state condition. The SCR TDZ profile may closely match the profile of the wall of a very shallow trench. However, for deeper trenches, the SCR TDZ, due to its high axial stiffness, cannot stretch enough to assume the trench wall profiles but follows its natural shape in equilibrium with the soft resistance provided by the loosed soil material in the trench, or overhangs if the loosed soil material are eroded from the trench. If the wave loads are high, the heave motions of the vessel will force the SCR TDZ deeper into the existing pre-trench, where the TDZ either follows the predefined trench shape upon having contact with the trench (Shiri 2014a) or digs deeper beyond the trench envelope. The deformation rate of the SCR TDZ will depend on a balance between the resistance of the loosed soil material in the trench or the resistance of virgin (unpenetrated) soil beyond the trench envelope and the global bending stiffness of the SCR TDZ. When the riser digs beyond the trench envelop under high amplitude motions, the trench tends to stabilise very quickly (Mekha, Randolph, Bhat and Jain 2013), defining a new/modified trench envelop. These interactions are very complex and drive the fluctuating SCR TDZ curvatures and the resulting fatigue damage. However, allowing these natural interactions of the SCR TDZ and the soil through comprehensive NL SCR-interaction models will provide more reliable results than enforcing a constrained artificial trenches envelopes as is done in many studies.

Although efforts are made in this paper to track these behaviours of the SCR TDZ fatigue damage in the considered pre-trench conditions, under the considered single applied wave load and direction, for the considered vessel motions, riser geometry, riser configurations, etc., the behaviours are quite complex and difficult to predict when any of these variables changed. For example, for a fully combined sea state fatigue wave conditions, typical of fatigue analysis plus second-order vessel effects, a simple prediction of the fatigue damage response in different pre-trench conditions is potentially elusive to common sense. However, with numerical tools and reliable methods, further investigation of the impact of these design variables can be conducted. For SCR design purposes, different scenarios involving combinations of varying design variables should be considered in sensitivity studies to increase design confidence that the presence of pre-trenches does not negatively impact the SCR response computed by the traditional method of SCR analysis with no pre-trench conditions.

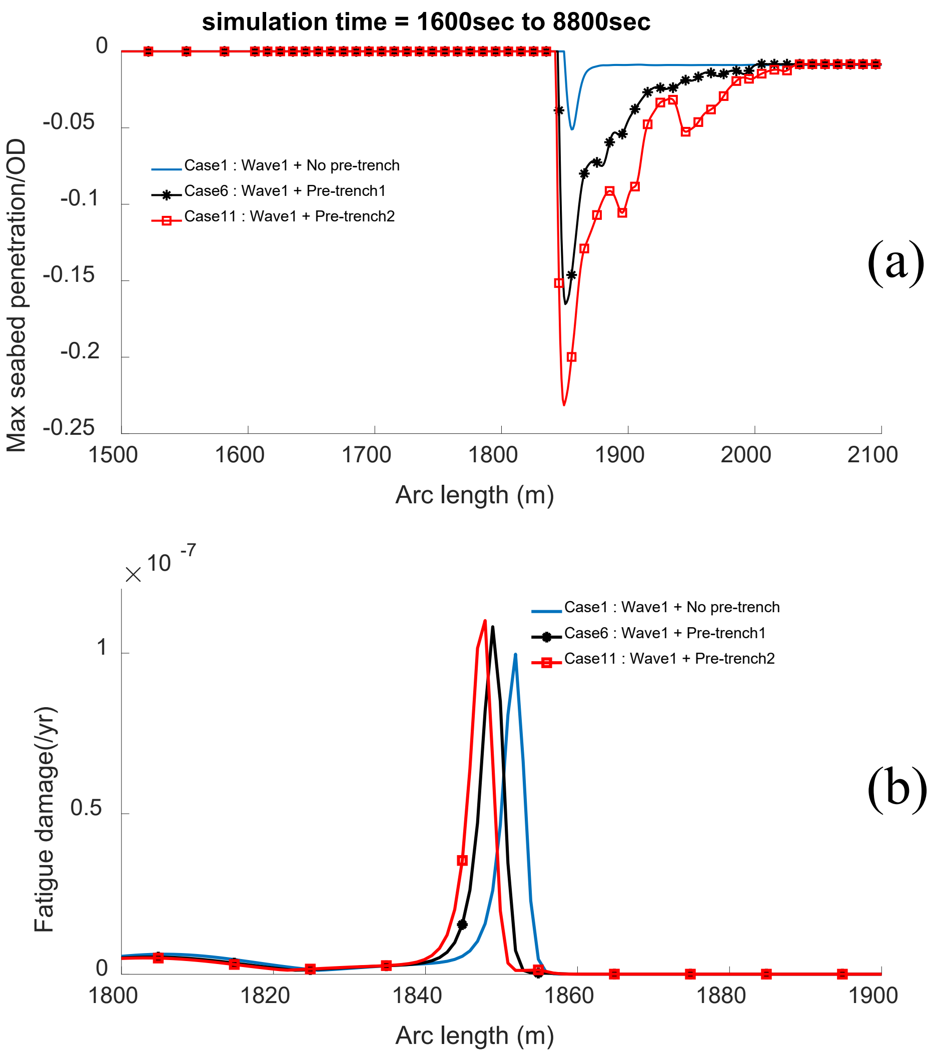

Figure 19 – (a) Final trench profile at the end of the main stage, (b) Fatigue damage response during the main stage for the three pre-trench conditions under wave1

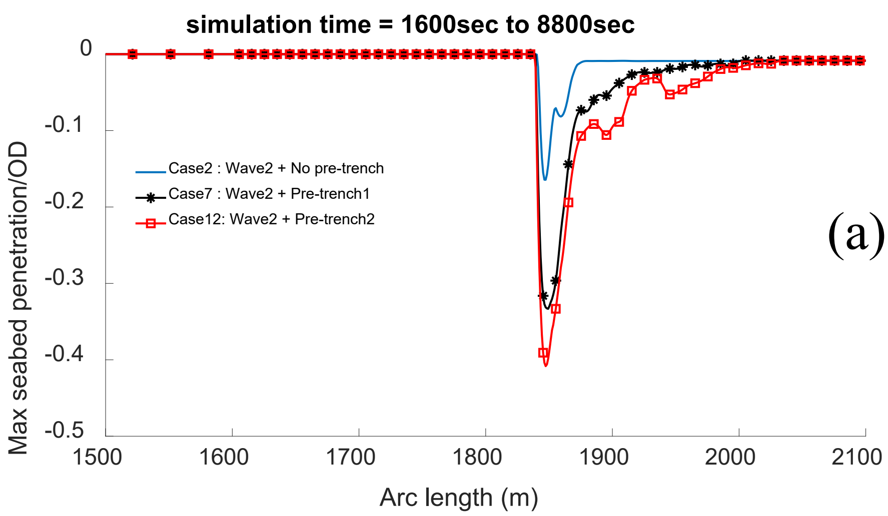

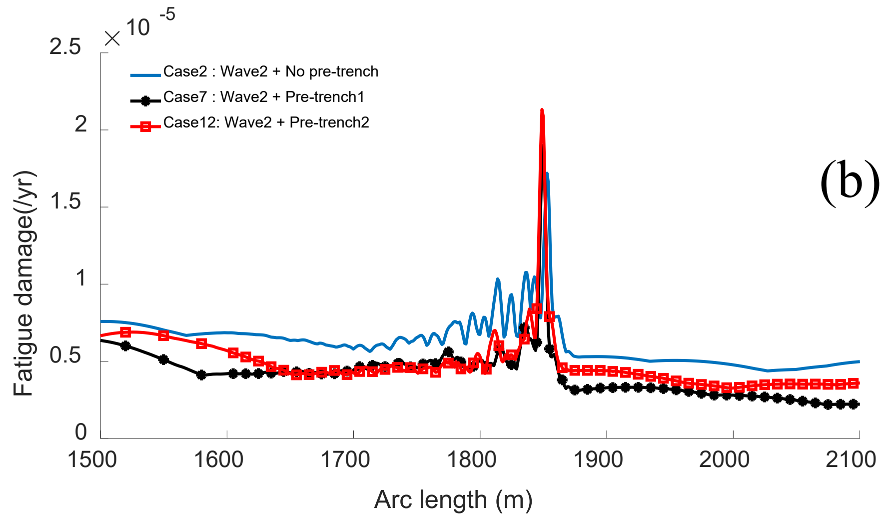

Figure 20 - (a) Final trench profile at the end of the main stage, (b) Fatigue damage response during the main stage for the three pre-trench conditions under wave2

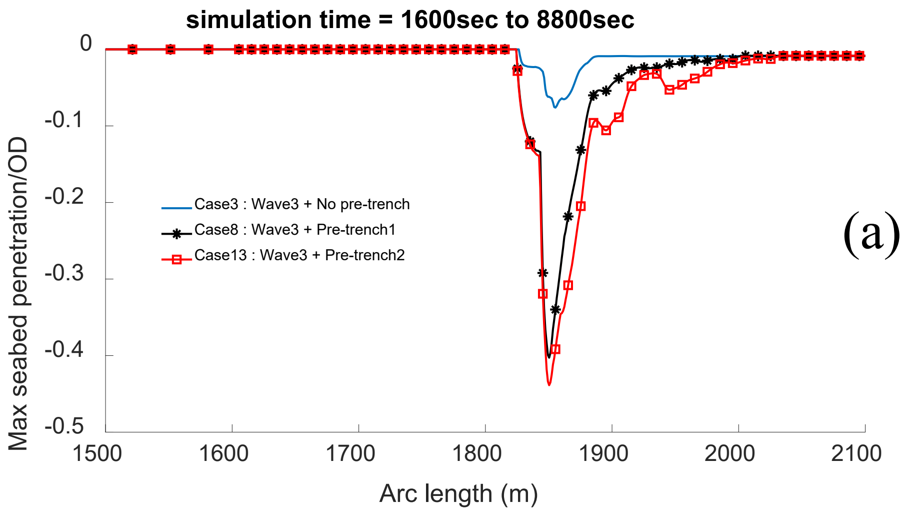

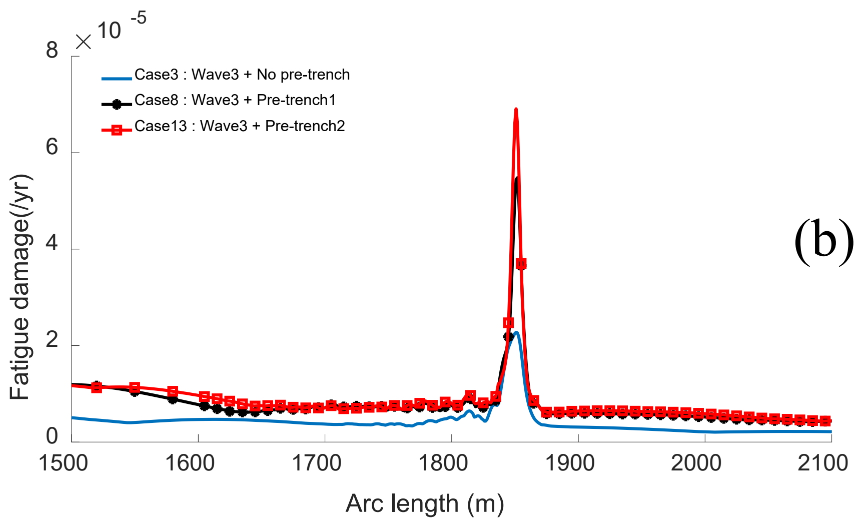

Figure 21 – (a) Final trench profile at the end of the main stage, (b) Fatigue damage response during the main stage for the three pre-trench conditions under wave3

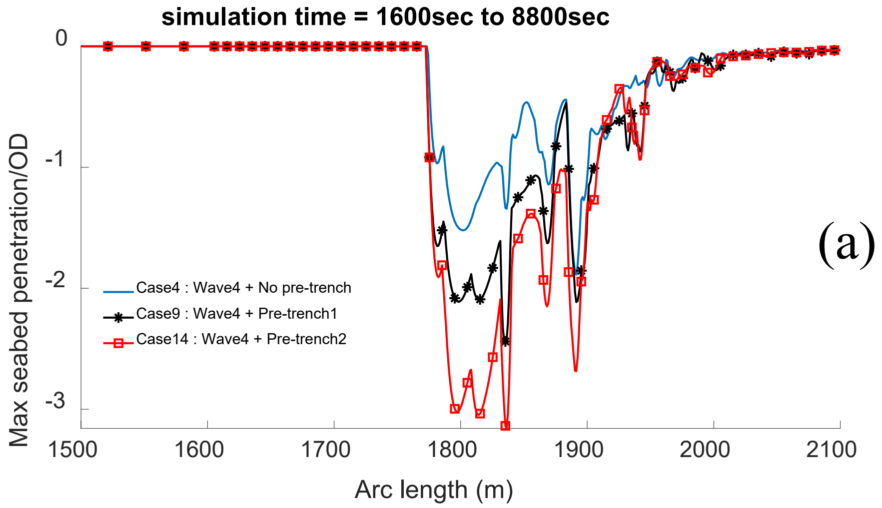

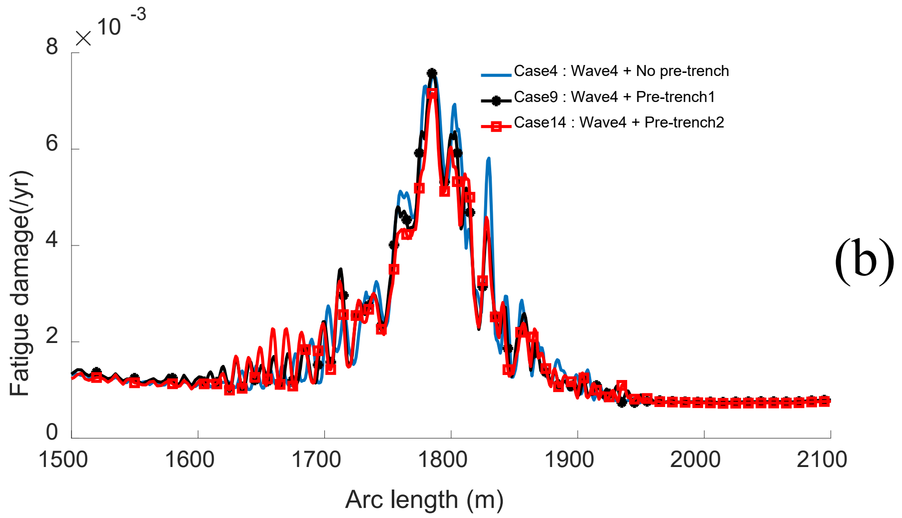

Figure 22 – (a) Final trench profile at the end of the main stage, (b) Fatigue damage response during the main stage for the three pre-trench conditions under wave4

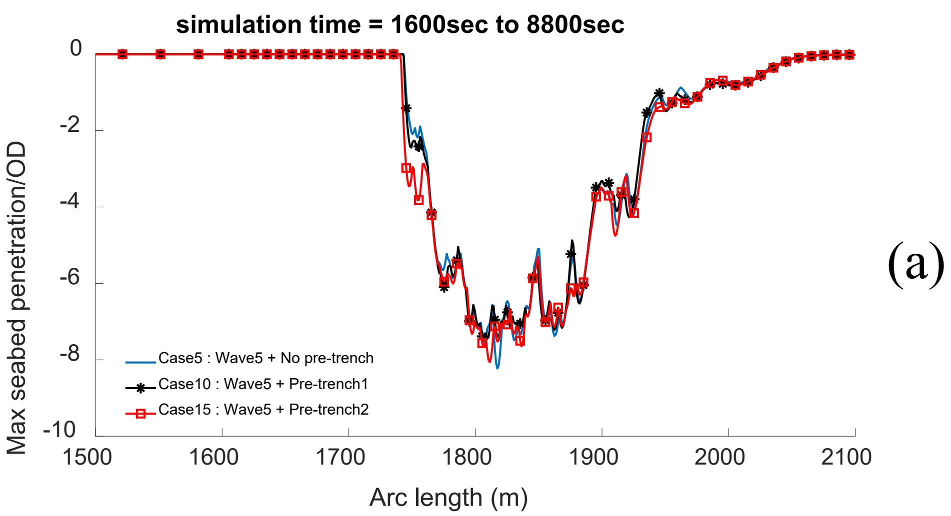

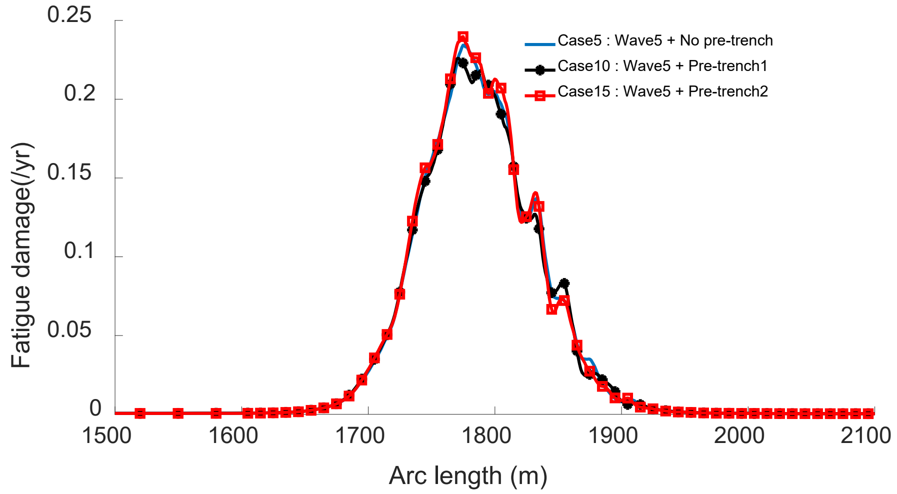

(b)

Figure 23 – (a) Final trench profile at the end of the main stage, (b) Fatigue damage response during the main stage for the three pre-trench conditions under wave5.

Table 8 – Summary of maximum SCR TDZ fatigue damage for the 15 analyses cases

	Pre-trench conditions		
Fatigue Loads	**No pre-trench**	**Pre-trench 1**	**Pre-trench 2**
Wave1 (Hs, Tp) = (1.5,5.5)	Case No: 1 Pre-trench = Static penetration Fatigue damage (/yr) = 9.97E-08	Case No: 6 Pre-trench = 2.04OD Fatigue damage (/yr) = 1.08E-07	Case No:11 Pre-trench = 4.49OD Fatigue damage (/yr) = 1.10E-07
Wave2 (Hs, Tp) = (3,8.8)	Case No: 2 Pre-trench = Static penetration Fatigue damage (/yr) = 1.72E-05	Case No: 7 Pre-trench = 2.04OD Fatigue damage (/yr) = 1.90E-05	Case No: 12 Pre-trench = 4.49OD Fatigue damage (/yr) = 2.13E-05
Wave3 (Hs, Tp) = (4.5,9.5)	Case No: 3 Pre-trench = Static penetration Fatigue damage (/yr) = 2.28E-05	Case No: 8 Pre-trench = 2.04OD Fatigue damage (/yr) = 5.48E-05	Case No: 13 Pre-trench = 4.49OD Fatigue damage (/yr) = 6.91E-05
Wave4 (Hs, Tp) = (8,13)	Case No: 4 Pre-trench = Static penetration Fatigue damage (/yr) = 7.58E-03	Case No: 9 Pre-trench = 2.04OD Fatigue damage (/yr) = 7.61E-03	Case No:14 Pre-trench = 4.49OD Fatigue damage (/yr) = 7.16E-03
Wave5 (Hs, Tp) = (15.8,16.9)	Case No: 5 Pre-trench = Static penetration Fatigue damage (/yr) = 2.34E-01	Case No:10 Pre-trench = 2.04OD Fatigue damage (/yr) = 2.26E-01	Case No: 15 Pre-trench = 4.49OD Fatigue damage (/yr) = 2.40E-01

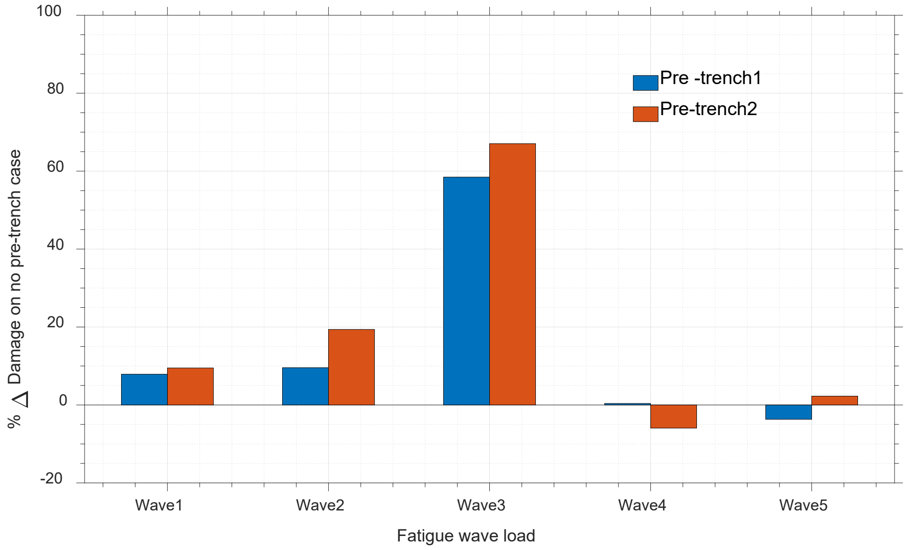

Figure 24 –Percentage change in fatigue damage of the pre-trench1 and pre-trench2 cases relative to the no pre-trench cases.

2.7. Pre-trench resistance and SCR TDZ bending moments

The pre-trench envelope is not an empty space or vacuum but contains softened soil caused by several cycles of SCR TDZ penetrations. Some of the loosed soil may be eroded and forced out of the trench by hydraulic- erosional processes from high water velocities as the pipe moves up and down into the trench (Clukey, Aubeny, Zakeri, Randolph, Sharma, White, Sancio and Cerkovnik). In such a case, overhanging of the SCR TDZ over a deep trench for calm conditions is a possibility. The strength of the soft soil is degraded compared to a virgin seabed that has not been penetrated. Although some authors indicate that the loosed soil, if left for a long period, can reconsolidate and regain appreciable strength (Hodder et al. 2009, Yuan et al. 2017), other authors suggested that the strength regained is significantly less than that before the seabed was penetrated (Aubeny et al. 2015, Clukey et al. 2008). However, the degradation of the seabed strength in stiffness and suction is captured by the RQ model (Randolph and Quiggin 2009).

To demonstrate that the soil materials within the pre-trench provide some form of resistance to the SCR TDZ motion, the range graph maximum of the seabed normal resistance per pipe diameter (OD) corresponding to the penetrations for case3 (wave3 + no pre-trench) and case8 (wave3 + pre-trench1) are presented in Figure 25 (a). Note that wave3 (H_s = 4.5m, T_p = 9.5sec) does not cause the SCR TDZ to exceed the pre trench1 envelope. This can be seen in Figure 18 (b), which is also presented in Figure 25 (a). It could be observed that the resistance imposed on the SCR TDZ by the pre-trench1 condition is significantly reduced compared to the seabed resistance imposed on the SCR TDZ for the no pre-trench condition (case3) under the same wave condition (wave3). This indicates that the pre-trench resistance is weakened after several penetrations of the pipe into the soil during the pre-trench stage. However, the maximum bending moments for these two cases are comparable, as seen in Figure 25 (b). The peak bending moment for case3 and case8 occur before the maximum penetrated point in the SCR TDZ. Although the maximum bending moment for both cases closely matched each other, the spatial variation of the bending moment along the SCR TDZ appears more random for the SCR TDZ section of the no pre-trench case (case3) and for the SCR TDZ section outside the pre-trench envelop for the pre-trenched case (case8), compared with section within the pre-trench envelope. This is the natural hot spots interactions of the SCR and seabed. Figure 25 (c) present the variation of fatigue damage with penetrations of the SCR TDZ section for both case3 and case8. Here it could be seen that since the SCR penetrated deeper into the pre-trench envelope for case8, compared with the no-pre-trench case (case3), more bending will be experienced by the SCR TDZ section of case 8 within the trench. Considering in Figure 25 (b), alongside within Figure 25 (c), it could be observed that the point of maximum bending moments (in these cases) do not coincide exactly with points of maximum fatigue damage. For both case3 and case8, the maximum fatigue damages occur at the most penetrated point of the SCR TDZ. This may imply that variation in the bending moment at the maximum fatigue damage point may have more influence on the fatigue damage than the amplitudes of the bending moments.

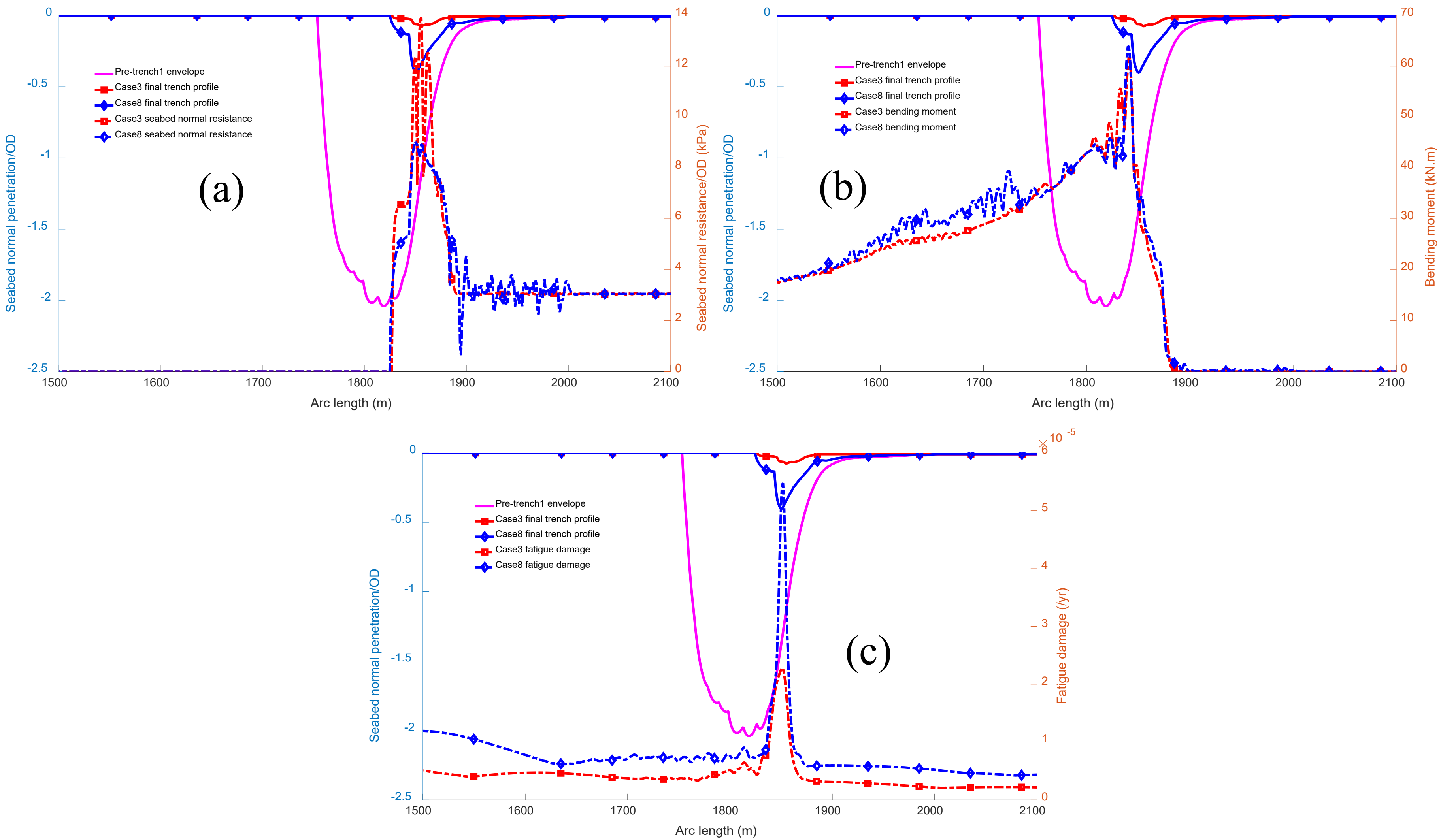

Figure 25 – (a) Seabed normal resistance to pipe penetration in the trench, (b) seabed normal penetration in comparison with SC TDZ bending moment.

Conclusion

It is essential to the riser industry to be able to qualify and quantify the fatigue damage response of the SCR TDZ in the presence of existing trench (pre-trench condition), complex fatigue wave load, vessel first order motions and vessel offsets in a full time-domain simulation. This knowledge will help the riser designer mitigate uncertainties surrounding the complex interactions between the SCR TDZ and the seabed. A new numerical pre-trenching technique, referred to as the simulation stage-based pre-trenching technique (SSBPT), is introduced in this paper to achieve this goal. The SSBPT decomposes the usual single simulation period into three stages which are the trenching stage (in which the pre-trench envelope is created), the rest stage (in which the pre-trenching load response are dampened out), and the main stage (in which the main fatigue wave load is imposed on the vessel-riser system in the presence of the created pre-trench). The SSBPT has been compared with similar studies developed on the same hysteretic non-linear soil interaction model but with a different pre-trenching approach. Although the two methods can provide pre-trenches, the SSBPT offers the opportunities to obtain longer span pre-trenches typical of those observed from field data by the imposition of oscilatory vessel offsets. This is possible due to the inclusion of oscillatory vessel offsets at the pre-trenching stage of the SSBPT. Also, though the peak fatigue damage occurs at a similar location for both techniques, the SSBPT can capture more spreading of the fatigue damage in the SCR TDZ neighborhood resulting from a combination of multiple fatigue wave loads of a broader range of amplitudes and periods.

The SSBPT has been demonstrated with an SCR example on which different random fatigue wave load conditions are imposed in the presence of different pre-trench conditions. The results indicate that the pre-trench can increase the SCR TDZ fatigue damage if the fatigue wave loads applied do not cause the SCR TDZ motions to exceed the existing pre-trench envelope. However, if the motions of the SCR TDZ caused by a combination of the wave load and the vessel response resulted in a trench, which exceeds the pre-trench envelope (longer and deeper), the resulting fatigue damage response will be similar (either larger or smaller) compared with the cases where a flat seabed or no pre-trench is assumed prior to the fatigue simulation. Since the trenching process is caused by other factors apart from the wave and vessel excitations, it is believed that the existing pre-trench envelope can fully accommodate the riser TDZ motions during the fatigue loading. Hence the pre-trench will likely cause an increase in the fatigue damage of the SCR TDZ section. However, if the pre-trench envelope is not able to accommodate the SCR TDZ large excitation, further trenching can be observed (referred to as trench in trench from the field observation study). The impact of this process can be captured by the SSBPT.

The fatigue load applied in this study is for one direction (along the riser azimuth), while the host vessel remains in its nominal position. Although the comparative study and the main analysis in this paper showed that pre-trenching increases the SCR fatigue damage, these interactions are too complex to make absolute conclusions. It is preferable to have suitable methods of accessing these interactions for a case-by-case investigation, which may not provide similar qualitative conclusions. A more robust understanding can be obtained with the SSBPT to investigate other variable conditions, such as different vessel motions, the vessel second-order offsets, the SCR global configurations, the SCR TDZ stiffness, different soil model data, different wave loads and directions etc. These will be covered in part-2 of the ongoing research work to help determine the net effect the pre-trench may have on the fatigue life or damage response of the SCR TDZ.

Acknowledgement

The authors acknowledge the support of the University of Strathclyde and McDermott International for sponsoring the research. Simulations in this work were facilitated by the use of ARCHIE-WeST High-Performance Computer (www.archie-west.ac.uk) based at the University of Strathclyde.

References

AS DNV. 2011. Fatigue design of offshore steel structures. Rev 3.

Aubeny C, White T, Langford T, Meyer V, Clukey E. 2015. Seabed stiffness model for steel catenary risers. Frontiers in offshore geotechnics III.351-356.

Aubeny CP, Biscontin G. 2009. Seafloor-riser interaction model. International Journal of Geomechanics.9:133-141.

Bridge CD, Howells HA. Observations and modeling of steel catenary riser trenches. Proceedings of the

The Seventeenth International Offshore and Polar Engineering Conference; 2007: International Society of Offshore and Polar Engineers.

Clukey E, Ghosh R, Mokarala P, Dixon M. Steel catenary riser (SCR) design issues at touch down area; 2007: International Society of Offshore and Polar Engineers.

Clukey EC, Aubeny CP, Zakeri A, Randolph MF, Sharma PP, White DJ, Sancio R, Cerkovnik M. A Perspective on the State of Knowledge Regarding Soil-Pipe Interaction for SCR Fatigue Assessments; 2017: Offshore Technology Conference.

Clukey EC, Young AG, Dobias J, Garmon S. Soil response and stiffness laboratory measurements of SCR pipe/soil interaction. Proceedings of the Offshore Technology Conference; 2008: Offshore Technology Conference.

Elliott BJ, Zakeri A, Barrett J, Hawlader B, Li G, Clukey EC. 2013. Centrifuge modeling of steel catenary risers at touchdown zone part II: Assessment of centrifuge test results using kaolin clay. Ocean Engineering. 2013/03/01/;60:208-218.

Giertsen E, Verley R, Schroder K. CARISIMA: A catenary riser/soil interaction model for global riser analysis. Proceedings of the ASME 2004 23rd International Conference on Offshore Mechanics and Arctic Engineering; 2004: American Society of Mechanical Engineers Digital Collection.

Gore CT, Mekha BB. 2002. Common Sense Requirements (CSRs) for Steel Catenary Risers (SCRs). Offshore Technology Conference, OTC.

Heffernan D. 2016. An introduction to the Python interface to OrcaFlex. Orcina, Tech Rep2016.

Hodder M, White D, Cassidy M. Effect of remolding and reconsolidation on the touchdown stiffness of a steel catenary riser: observations from centrifuge modeling. Proceedings of the Effect of remolding and reconsolidation on the touchdown stiffness of a steel catenary riser: observations from centrifuge modeling; 2009: Offshore Technology Conference.

Langner CG. 2003. Fatigue Life Improvement of Steel Catenary Risers due to Self-Trenching at the Touchdown Point. Offshore Technology Conference, OTC.

Matsuishi M, Endo T. 1968. Fatigue of metals subjected to varying stress. Japan Society of Mechanical Engineers, Fukuoka, Japan.68:37-40.

Mekha B, Randolph M, Bhat S, Jain S. Modeling the Touchdown Zone Trench and Its Impact on SCR Fatigue Life. Proceedings of the Offshore Technology Conference; 2013: Offshore Technology Conference.

Nakhaee A, Zhang J. 2008. Effects of the Interaction With the Seafloor On the Fatigue Life of a SCR. The Eighteenth International Offshore and Polar Engineering Conference, ISOPE.

Orcina L. 2018. OrcaFlex User Manual: OrcaFlex Version 10.2 c. Daltongate Ulverston Cumbria, UK.

Quéau LM, Kimiaei M, Randolph MF. 2015. Sensitivity studies of SCR fatigue damage in the touchdown zone using an efficient simplified framework for stress range evaluation. Ocean Engineering.96:295-311.

Quintin H, Legras J-L, Huang K, Wu M. Steel catenary riser challenges and solutions for deepwater applications. Proceedings of the Offshore technology conference; 2007: Offshore Technology Conference.

Randolph M, Quiggin P. Non-linear hysteretic seabed model for catenary pipeline contact. Proceedings of the ASME 2009 28th International Conference on Ocean, Offshore and Arctic Engineering; 2009: American Society of Mechanical Engineers.

Rezazadeh K, Shiri H, Zhang L, Bai Y. 2012. Fatigue generation mechanism in touchdown area of steel catenary risers in non-linear hysteretic seabed. Research Journal of Applied Sciences, Engineering and Technology.4:5591-5601.

Sharma PP, Aubeny CP. Advances in pipe-soil interaction methodology and application for SCR fatigue design. Proceedings of the Offshore Technology Conference; 2011: Offshore Technology Conference.

Shiri H. 2014a. Influence of seabed trench formation on fatigue performance of steel catenary risers in touchdown zone. Marine Structures.36:1-20.

Shiri H. 2014b. Response of steel catenary risers on hysteretic non-linear seabed. Applied ocean research.44:20-28.

Shiri H, Randolph M. 2010. The Influence of Seabed Response on Fatigue Performance of Steel Catenary Risers in Touchdown Zone.63-72.

Shoghi R, Shiri H. 2019. Modeling touchdown point oscillation and its relationship with fatigue response of steel catenary risers. Applied Ocean Research.87:142-154.

Shoghi R, Shiri H. 2020. Re-assessment of trench effect on fatigue performance of steel catenary risers in the touchdown zone. Applied Ocean Research.94:101989.

Song R, Stanton P. Advances in Deepwater Steel Catenary Riser Technology State-of-the-Art: Part I—Design; 2007: American Society of Mechanical Engineers.

Veritas DN. 2010. Recommended practice DNV-C203: Fatigue design of offshore steel structures. In: DNV Oslo.

Wang K, Low YM. Study of seabed trench induced by steel catenary riser and seabed interaction. Proceedings of the ASME 2016 35th International Conference on Ocean, Offshore and Arctic Engineering; 2016: American Society of Mechanical Engineers Digital Collection.

Yuan F, White D, O'Loughlin C. 2017. The evolution of seabed stiffness during cyclic movement in a riser touchdown zone on soft clay. Géotechnique.67:127-137.

Zargar E, Kimiaei M, Randolph M. 2019. A new hysteretic seabed model for riser-soil interaction. Marine Structures.64:360-378.